THEORY AND PRACTICE OF BRINE PROCESSING BY INDUSTRIAL-SCALE MAGNETIC ION POLARIZATION AND OPTIMIZATION OF PERSONAL-SCALE PASSIVE SOLAR DESALINATION

by

MICHAEL HENRY WOFSEY

A DISSERTATION

Submitted in partial fulfillment of the requirements
for the degree of Doctor of Philosophy in the
Department of Physics and Astronomy
in the Graduate School of
University of Alabama

TUSCALOOSA, ALABAMA

2010

ABSTRACT

In the first section of this work we hope to add to the science of brine management in desalination. We have undertaken a feasibility analysis of a method of brine processing where the ions in solution are transported by an axial magnetic field in a long pipe, and an off-center cross-section of the flow is extracted with a lower ion concentration than that near the edges of the pipe. We constructed an apparatus that examines this process and allows us to measure the change in voltage in a solution during treatment. The goal of this process is to separate brine effluent from the desalination system into two components; one close to ocean water which can be safely injected back into the ocean or reprocessed into potable water using standard desalination techniques. The second component will have an ion concentration higher than typical waste brine, and can be more economically treated using a conventional process such as an evaporation pond or solar drying.

This research addresses an emerging problem, the Achilles' heel of large-scale desalination. Specifically, systems for municipal-sized water demands can produce desalinated water in quantities exceeding a million liters per day. A basic mass balance shows that all the freshwater that is extracted from seawater will leave a nearly equal quantity of high-salt brine. Ejected brine from commercial-scale desalination facilities has been shown to cause distress and damage to marine organisms and possibly even saline gradient inversions, which lead to unpredictable solar heating of littoral ocean waters.

In the second section of this work we add to the general knowledge of the science of solar desalination. We have used common and straightforward measurement techniques, physical analyses and quantitative analyses to optimize efficient methods of personal-scale solar desalination. In this research we have used simple modifications to stills of our own design that increase efficiency and output of distilled water. We also examine a theoretical efficiency model that may be useful in determining the efficiency of solar stills and offer potential predictor of solar still output efficiency.

DEDICATION

This dissertation is dedicated to people who have experienced loss due to drought and unsafe drinking water. I am thankful to Jennifer, Lilly, Willow, Flora, David, Tammy and Eden for their patience and support.

LIST OF ABBREVIATIONS

AC	Anti-condensate
DSSB	Double slope single basin
FPP	Flexible polyethylene panels
GMR	Giant magnetoresistance
LFIP	Lorentz force ion polarization
MSFD	Multi-stage flash distillation
PPM	Parts per million
PSPSD	Personal-scale passive solar desalination
PSS	Passive solar still
PSSD	Personal scale solar desalination
PVC	Polyvinyl chloride
PVF	Polyvinyl fluoride
RAP	Rigid acrylic panels
RO	Reverse osmosis
SBSS	Single basin single slope
SEA	Solar Evaporation Array
SIM	Solar incident meter

SLS	Sodium lauryl sulfate
SSSB	Single slope single basin
SWRO	Seawater reverse osmosis
TDS	Total dissolved solids

ACKNOWLEDGEMENTS

I thank Professor Richard Tipping for patient guidance and research on this work, and the dissertation committee for their help with various questions and problems and evaluation of this work.

Professor Martin Bakker

Professor James W. Harrell

Professor Patrick Leclair

Professor Gary Mankey

U.S. Environmental Protection Agency for their support of this work through their E.P.A. P3, Phase I, sustainability grant.

Economic Development Partnership of Alabama and Alabama Launchpad Consortium for their generous support of this research, with ALC Director Glenn Kinstler.

University of Alabama Office of Technology Transfer for their generous help in securing necessary U.S. Patents from this research.

University of Alabama Department of Physics and Astronomy for their gracious support.

University of Alabama Institute for Manufacturing Excellent for their generous use of facilities.

CH2M Hill and the Australian National Centre of Excellence in Desalination for including elements of this work in design of their technical trial facility in Western Australia.

SEA Desalination, Corp., for the use of their facilities and purchase of necessary equipment related to this research.

CONTENTS

LIST OF TABLES

LIST OF FIGURES

CHAPTER 1

GENERAL INTRODUCTION

This dissertation combines two distinct areas of research, both aspects of the physics and science of desalination. Section I deals with a potential industrial method of managing the problem of brine effluent from desalination plants. This is early-stage feasibility research and construction of a pilot scale operation to test these principals is far beyond our resources. However Section II covers actual personal-scale solar desalination units, complete with field-testing and optimization.

These two areas differ widely in cost of implementation. While the brine treatment method may well cost upwards of a million dollars to produce a pilot scale operation, the personal-scale desalination units have been conceived, developed and brought to market for a fraction of that cost, thus the reason we have field data from these units. Both areas of research are related in that they attempt to solve the real life problems of water supply and the ensuing environmental impact of creating potable water from seawater. While the two areas of research are independent of each other, we hope that their inclusion in the same dissertation draws attention to not only the present needs of desalination but also the potential for future problems with desalination; specifically that in high concentrations NaCl is toxic and its disposal needs to be considered. The industry and science of desalination is growing at such a rate that its importance in our future seems guaranteed. We hope that the proper and considered disposal of the removed salt will also be part of that future.

SECTION I

CHAPTER 2

LORENTZ FORCE ION POLARIZATION

2.1 Justification

A key area of research in desalination is management of waste concentrate. The two most common methods of desalination (reverse osmosis and flash distillation) are not capable of removing all the pure water from a saltwater or contaminated source and must discharge up to 50% of their input as concentrate [1]. Current and emerging methods can be classified into two general methods in the treatment of the waste stream: dilution and concentration. Dilution methods are most common, and these methods include discharge of the waste concentrate into ocean, river, lake, deep well, and sewer or irrigated onto land. These methods currently account for disposal of over 90% of all desalination facilities in the U.S. [2]. The other existing method of managing concentrate is to evaporate all or most of the water from the concentrate leaving behind a solid or slurry, which has a much lower total mass than the brine. This is then crystallized with either an outdoor (solar) evaporation pond or by using an industrial method such as thermodynamic evaporation. The power demands for these latter methods are often higher than the cost of the desalination process itself.

Of the existing methods, dilution is commonly used because it is economical. However, dilution can often have the drawback of causing environmental damage due to the salt concentrates contaminating groundwater supplies, harming irrigable land, or harming marine organisms that are not tolerant to elevated salinity.

There are emerging methods that aim to enhance the problems of concentrate management, many of which show promise from a technical point of view as outlined in Sethi et al. [1]. These methods typically either increase the efficiency of the osmosis process, which leads to less total mass of concentrate, or else they are novel methods of desalination that lead to near-zero liquid discharge of brine, and allow the salt and contaminants to be removed as solids or a salt slurry.

2.2 Background of industrial-scale ion polarization

This research suggests a different approach. We start from the assumption that direct discharge of concentrate – given its current widespread use due to low cost – will likely be a common brine management method for many years to come. We then hope to use experimentation and theory to examine the feasibility of a long pipe treatment process where the discharge with high total dissolved solids (TDS) can be magnetically treated to break the effluent into two waste streams, one with a salt concentration very close to seawater (i.e. around 35,000 parts per million (PPM)) and one with much higher salt concentration, for instance up to half total mass in salt or higher. This would allow the much larger 35,000 PPM stream to be discharged back into the ocean (or the effluent can be salinity-matched to brackish conditions in bays and rivers) and the high-salt slurry to be economically disposed of, or crystallized to a co-product using outdoor or industrial evaporation methods.

Our electromagnetic approach examines the possibility of using motional (or Faraday) voltages due to the Lorentz force, $\mathbf{F} = q\mathbf{E} + (q\mathbf{v} \times \mathbf{B})$. This was examined in a flowing electrolyte by Wright and Van Der Beken in 1972 [3]. In their experiment, they

demonstrate that saltwater moving through a magnetic field (but with just a $(q\mathbf{v} \times \mathbf{B})$ and not a $q\mathbf{E}$ contribution) experiences a force that separates the positive and negative ions and sets up an electric field measurable by the potential difference across the flow tube. The authors specifically pointed out that this effect is different from the conventional semiconductor Hall effect since unlike charges are moving in the same direction and thus experience opposite forces. With the Hall effect in semiconductors, the charges (i.e. holes and electrons) move in opposite directions in the semiconductor and thus experience a Lorentz force in the same direction. Driver in 1978 [4] pointed out that the effect observed by Wright and Van Der Beken is not due to the Hall effect in any way, but rather just the Faraday voltage from the Lorentz force. [Figure 2.2.1]

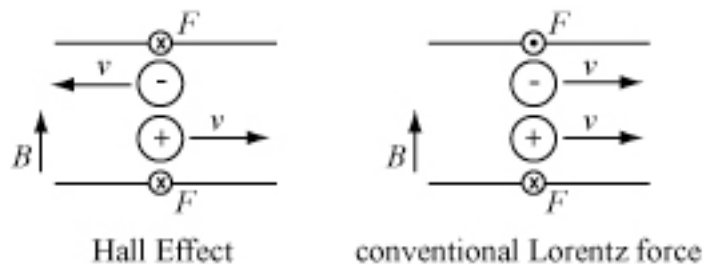

Figure 2.2.1 Comparison of Hall Effect to conventional Lorentz force

De Luca examined this effect more recently in 2009 [5]. In De Luca's theoretical analysis, salt water flows through a rectangular pipe under the influence of a transverse magnetic field. The resulting Lorentz force gives rise to the Faraday voltage on electrodes at the end of the pipe. This analysis then examines the chemical reactions at the cathode and anode. Specifically, at the cathode, water is electrolyzed and hydrogen gas is produced, and at the anode chlorine gas is produced. The desire to exploit this effect for the purpose of desalination is examined in at least one U.S. Patent [6].

Our experiment differs from these in that we use the $(q\mathbf{v} \times \mathbf{B})$ contribution to the Lorentz force with a relatively low-strength magnetic field (with direction transverse to the direction of fluid flow) over a long flow distance to examine a feasible method for the treatment of brine concentrate as outlined earlier. Given the limitations of our apparatus and instrumentation, we did not set up to measure a change in salinity across a section of the flow, however we used our electrical measurements to examine the feasibility of eventually constructing a full-scale magnetic separation device which will process brine as described above.

Very recent research in the area of ion polarization by a group at MIT has produced a workable device using the effect of ion concentration polarization for direct desalination of seawater [7]. This research exploits ion depletion in a microscale device using a cation exchange membrane. They use small flow channels, in the 100 micrometer domain, with ion control through a nanojunction. Using natural seawater taken from Crane Beach in Ipswitch, MA, the device is reported to have achieved over 99% removal rate. Our research differs from this work in that we intend to examine this method using conventional industrial pipe diameters, fluid flow and centimeter scale, and that the ion polarization with our technique is a result only of the transverse magnetic field with work supplied by the fluid flow.

2.3 Previous attempts

Before examining our current method (Fig. 2.3.1, page 9) , we briefly describe our previous attempts at ion polarization. Our first attempt used the force from the electric field only, with an approximately 3 meter long tube with an electrode at each end of the

tube (Fig 2.3.2, page 9). Potential differences axial to the direction of the tube were measured at each end and in the center of the tube. There was no flow in the tube and voltages from 10 to 1000 volts were supplied. Our goal was to polarize the ions through the length of the tube, and then draw off some solution at the center and see if we were able to reduce the PPM of the solution that we put in the tube. This experiment showed a result that was likely noise, with no correlation with theory, although ion capacitance is an active area of research where aerogels are used to adsorb ions in solutions with an applied electric field. Our second experiment used a small magnetic field of about a hundred Gauss, applied over a small distance of about 6 cm, below and above a three way junction (Fig 2.3.3, page 10), and the theory is given in the next section, although this experiment did not produce a significant result either.

After this we examined using a magnetic field along with our electric field on an open race of approximately 2 meters, with a three-port selector at the end (Fig 2.3.4, page 10), again with no result. Our next attempt was to reuse the pipe apparatus from our first experiment but with the added wire loops to create a magnetic field along with the electric field (Fig 2.3.5, page 11). We achieved results but were unable to correlate them with our theory. We began to suspect that our problem was the electric field, so we then created an apparatus with a much larger surface area for the electrodes, and used steel mending plates which are commonly used in construction and are composed of essentially many extruded nails on a metal plate (Fig 2.3.6, page 11), with scores of needles interweaving each other (but not touching). We hoped that even a fairly small amount of voltage would be able to polarize the ions given the more favorable geometry of this system. In this case, the water we removed during treatment was always higher in

total dissolved solids, clearly a negative result. We continually cut our applied voltage, and were surprised to find that even with no voltage applied, the output water from the device still had a slightly higher PPM than the source. We ultimately concluded that even without applied voltage, the saltwater corroded the steel electrodes and added dissolved solids to the total mixture. Due to this, we concluded that without specialty electrodes (like aerogels) that corrosion will be a common problem and direct contact with metal parts should be avoided for seawater. All of our tests resulted in overall higher PPM after electric treatment, which seems to be explainable by material from the electrodes entering solution. This led us to look at the Lorentz Force using magnetic fields only (Fig 2.3.7, page 11), on which the rest of our results are based.

The advantages with using only applied magnetic fields are compelling; specifically that the solution can stay in contact only with the nonreactive PVC piping, where corrosion from the saltwater is not a problem. Our first attempt in this area was to provide an applied magnetic field above and below a three-way fluid union and recirculate the solution continuously through this union. The concept was that each side diversion (left and right) that flowed through the transverse magnetic field would carry a larger number concentration of positive and negative ions, which would leave the center diversion somewhat diminished of ions, and thus this would demonstrate a lower PPM. Unfortunately, our applied magnetic field was not strong enough, our transverse distance was too small, and we could not measure a significant voltage difference, which would have indicated ion polarization.

Given this small distance, we then constructed an apparatus with a longer length, approximately 2 meters, with the magnetic field supplied by longitudinal windings

around a long fluid race, with a three gate diversion at the end, the left and right sides recirculating, and the center diversion collected and measured for PPM of the treated concentrate. Again, we were not able to detect a result. After reexamination of our calculations we understood that the effect would still be too small to measure. Our final test produced the results we examine in this research, which will be described in subsequent sections. A rough schematic of the apparatus is shown in Fig. 2.3.1.

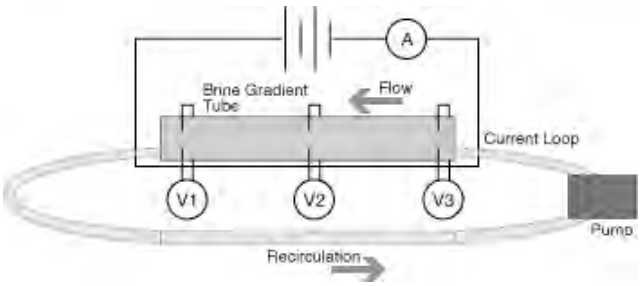

Fig. 2.3.1 Schematic of Lorentz force ion polarization test unit.

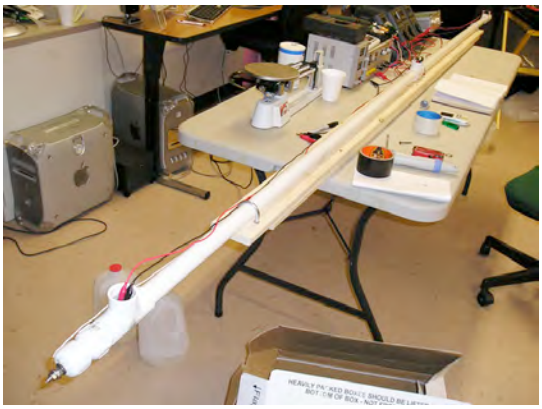

Figure 2.3.2 Unsuccessful attempt using electric force

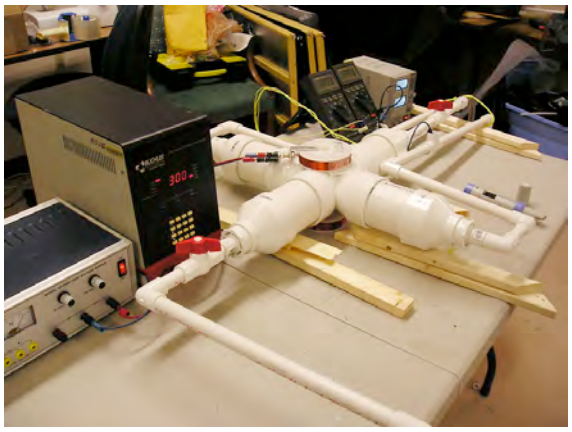

Figure 2.3.3 Unsuccessful attempt using magnetic force over a small distance

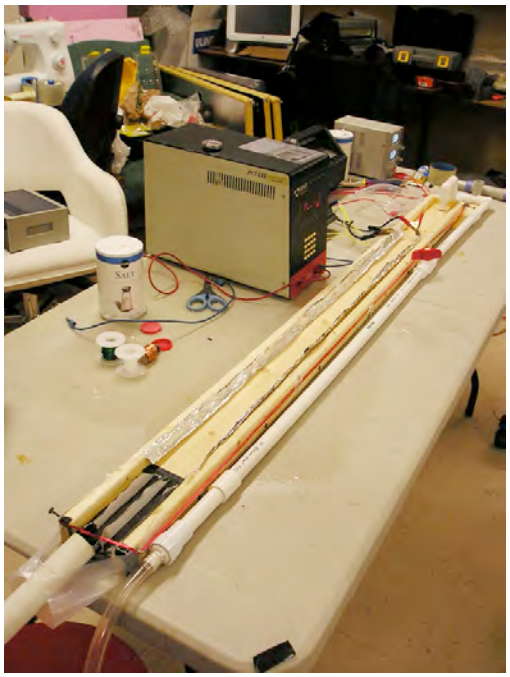

Figure 2.3.4 Unsuccessful attempt using magnetic force over an open race

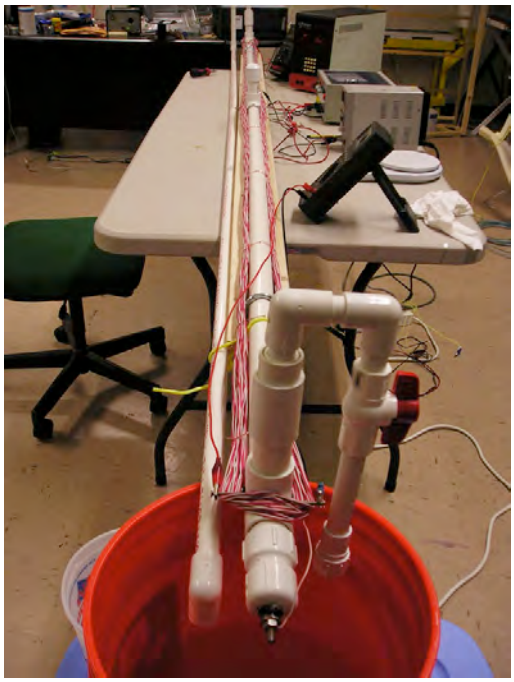

Figure 2.3.5 Unsuccessful attempt using both electric and magnetic forces

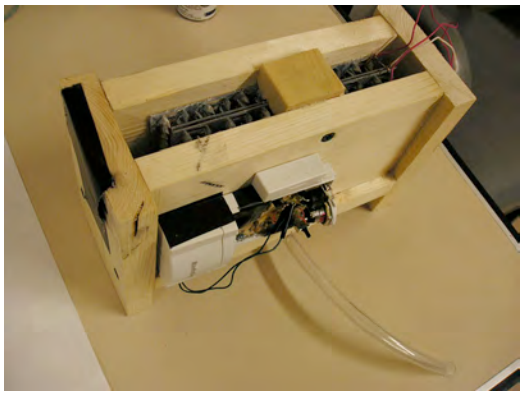

Figure 2.3.6 Unsuccessful attempt using electric force with high-area cathode/anodes

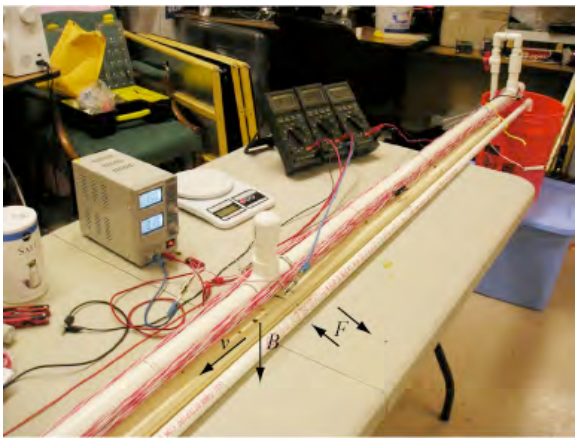

Figure 2.3.7 Successful attempt using magnetic force over a long distance

CHAPTER 3

LORENTZ FORCE ION POLARIZATION (LFIP) THEORY

As the salt solution flows through the pipe with an applied magnetic field as described, the ions experience a force **F**. *What are the parameters necessary to get an ion flowing in the center of the pipe to move toward the edge at the end of the pipe so that it can be separated from the fluid stream?*

The drag force on an ion for very small Reynolds numbers (below approximately 2400) in a continuous viscous fluid with laminar flow can be accurately modeled by Stokes law [8], which gives the drag force as $F_{\mathrm{D}} = 6\pi\eta R v$, where η is a fluid's dynamic viscosity, R is the Stokes radius of the ion, and v is the ion's velocity component normal to the direction of fluid flow, i.e. across the flow. (The ion's velocity *along* the fluid flow is roughly constant at v_y.) [Figure 3.1]

$$F_{\mathrm{L}} - F_{\mathrm{D}} = ma = m\frac{dv}{dt}. \qquad \text{(Eq. 3.1)}$$

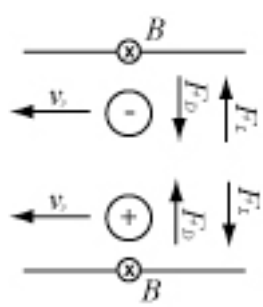

Figure 3.1 Orientation of forces in pipe

Using Stokes law and the Lorentz force, $F_{\mathrm{D}} = 6\pi\eta R v$, and $\mathbf{F}_{\mathrm{L}} = q\left(\mathbf{v}_{\mathrm{y}} \times \mathbf{B}\right)$. Since the magnetic field acts transverse to the direction of flow, $F_{\mathrm{L}} = qBv_y$ where q is the

charge on an ion, **B** is the magnetic field vector, and v_y is the constant velocity of the ion in the fluid flow transverse to the magnetic field. Substituting into (Eq. 3.1),

$$qBv_y - 6\pi\eta Rv = m\frac{dv}{dt}, \qquad \text{(Eq. 3.2)}$$

dividing through by m,

$$\frac{qBv_y}{m} - \frac{6\pi\eta R}{m}v = \frac{dv}{dt} \qquad \text{(Eq. 3.3)}$$

then assigning variables, $a \equiv \frac{qBv_y}{m}$ $b \equiv \frac{6\pi\eta R}{m}$. Thus,

$$a - bv = \frac{dv}{dt}. \qquad \text{(Eq. 3.4)}$$

Solving this differential equation by separating variables,

$$\int dt = \int \frac{1}{a - bv}\, dv, \qquad \text{(Eq. 3.5)}$$

solving and simplifying,

$$-b(t + c) = \ln(a - bv), \qquad \text{(Eq. 3.6)}$$

where c is a constant of integration, which leads to,

$$v = \frac{a - e^{-b(t+c)}}{b}. \qquad \text{(Eq. 3.7)}$$

Applying the boundary condition where at t=0, v=0, we find that

$$c = -\frac{\ln(a)}{b}, \qquad \text{(Eq. 3.8)}$$

and thus,

$$v = \frac{a - e^{\ln(a) - bt}}{b} = \frac{a - ae^{-bt}}{b}. \qquad \text{(Eq. 3.9)}$$

Substituting for a and b, we get

$$v = \frac{qBv_{\mathrm{y}}}{6\pi\eta R}\left(1 - e^{-\frac{6\pi\eta R}{m}t}\right). \qquad \text{(Eq. 3.10)}$$

This is the speed of the ion across the fluid flow. For a given flow rate *f* and cross-sectional pipe area πr^2, the velocity of fluid in the pipe is $v_{\mathrm{y}} = f/\pi r^2$. For our setup, (where length $l \gg r$*),* the magnetic field is determined from the applied current *I*, μ, the permeability of the electromagnet core (water), *N* the number of current-carrying wire turns and, thus $B = N\mu I/\pi r$. Substituting these into (Eq. 3.10),

$$v = \frac{qN\mu fI}{6\pi^3\eta R}\frac{If}{r^3}\left(1 - e^{-\frac{6\pi\eta R}{m}t}\right) \qquad \text{(Eq. 3.11)}$$

As the Lorentz force $\mathbf{F}_{\mathrm{L}}$ increases, the velocity component of the ion *v* increases, eventually $\mathbf{F}_{\mathrm{L}} = \mathbf{F}_{\mathrm{D}}$, and the ion moves with a speed v_{terminal} and zero acceleration across the flow, therefore,

$$v_{\mathrm{terminal}} = \frac{qN\mu}{6\pi^3\eta R}\frac{If}{r^3}. \qquad \text{(Eq. 3.12)}$$

The terminal velocity is fairly slow, on the order of 1 cm/s for a pipe diameter of 2.5 cm. Given the length of the pipe, it is reasonable to neglect the small acceleration time to terminal velocity.

Using kinematics to move an ion from the center of the laminar flow through a distance *r* to the edge of the pipe requires a time $t \simeq r/v_{\mathrm{terminal}}$. The time that the ion spends in the pipe in the B field is determined by the length *l* of the pipe, and the longitudinal flow velocity through the pipe. The fluid spends a time in the pipe of $t = lA/f$, where *l* is the length of the pipe, *A* is the cross-sectional area, and *f* is the flow in units of volume per unit time. Therefore, $lA/f = r/v_{\mathrm{terminal}}$ and one can write,

$$\frac{l}{d^2} = \frac{3\pi^2 \eta R}{2q\mu IN}, \qquad \text{(Eq. 3.13)}$$

where d is the diameter of the pipe.

The use of R as the Stoke's radius of the ion can be improved since the ion essentially carries a hydration sphere of roughly $3R$, when the surrounding water molecules are considered. Thus, accounting for the hydration sphere, (Eq. 3.13) becomes,

$$\frac{l}{d^2} = \frac{9\pi^2 \eta R}{2q\mu IN}. \qquad \text{(Eq. 3.14)}$$

The requirements to migrate an ion to the side of the pipe are not dependent on the flow velocity, *assuming a nonzero flow*. Rather (with a given number of turns N of current-carrying wire) this requirement is dependent on the supplied current, length of the pipe and the inverse square of the pipe diameter.

We have not considered in this analysis the repulsive force experienced by the ion when it moves to the edge and interacts with other same-charge ions (with higher number density) than in the volume. This extended analysis will require further work, but given the scale of an industrial pipe and the inverse-square relationship of the repulsive force between like charges, we expect this to be a good estimate for small number concentrations of ions. Also, there is an electrical attraction between oppositely-charged ions in the polarization, but as with the like-charge repulsion, this effect drops off with the inverse-square of the distance between charges, so while the attractive force will serve to resist the polarization just as the repulsive force will, its effect will be smaller.

CHAPTER 4

LFIP APPLICATION

4.1 Feasible configuration

The goal of the preceding analysis it to find the feasibility of ion polarization on a centimeter-scale using magnetic fields. This process is feasible if certain constraints are applied, and completely unfeasible if those constraints are not applied. For instance, we rewrite (Eq. 3.14) derived with straightforward constraints as,

$$\frac{NIl}{d^2} = \frac{9\pi^2 \eta R}{2q\mu}, \qquad \text{(Eq. 4.1.1)}$$

with the constants in the equation as follows, (given that the magnetic permeability of freshwater is very close to that of a vacuum) as applied to salt water viscosity, given ion size, and charge:

$$\begin{aligned} \mu &= 1.26 \times 10^{-6}\ \mathrm{H \cdot m^{-1}} \\ R &\simeq 1.35 \times 10^{-10}\ \mathrm{m} \\ q &= 1.60 \times 10^{-19}\ \mathrm{C} \\ \eta &= 1.08 \times 10^{-3}\ \mathrm{Pa \cdot s}\ , \end{aligned}$$

We find for our values of *N, I,* and *d* that the necessary length *l* to achieve near complete polarization (neglecting like charge repulsion) is nearly $3 \times 10^8\ \mathrm{m}$, nearly the distance from the Earth to the Moon. Clearly, a pipe that long would be difficult to build. However, we only need a fraction of this performance to create a functioning brine processing system, and we can improve the operating parameters.

As seen from (Eq. 4.1.1) *I, l, N*, all contribute linearly and *d* as the inverse square. We can increase our input amperage ten-fold by using 10-gauge wire rather than 20-

gauge wire, or increase the number of turns *N*. Further, our goal is to reduce high-salt brine to standard-salinity ocean water, so we don't need complete ion polarization. To reduce brine that is approximately 60,000 PPM to approximately 30,000 PPM seawater we can effectively consider half the distance, since we only need half of the effective polarization. These relaxed criteria still require a very long pipe, but we can use a long oval race, and then continually move the same volume of solution around the race to achieve an effective linear distance. When the desired polarization has been achieved, the water can then be diverted into three flows: a center flow and two side flows. The two side flows will be ion-heavy and can be recombined into a salt brine with higher PPM than the original solution, and the center flow can be extracted and reintroduced to the ocean, desalinated using standard techniques or reprocessed with the same technique until the desired salinity is reached.

Further, it will probably be advantageous to separate the flow into *M* number of multiple pipes. For a given desalination plant with freshwater output *W* in cubic meters, the brine output is approximately equal to the freshwater output. This volume is $W = \pi d^2 l/4$. Solving for π and inserting into our necessary pipe length,

$$l = \frac{1}{M}\left[\frac{72\eta R}{q\mu IN}\frac{W^2}{d^2}\right]^{1/3}. \qquad \text{(Eq. 4.1.2)}$$

We see that necessary length is reduced with increased pipe diameter. Using our aforementioned constraints but with a pipe diameter of 10 cm, we find that the necessary length for a $W = 1{,}000\ \mathrm{m}^3$, and total number of pipes $M = 1{,}000$ and taking half of the total length for reduction of brine to salt concentration similar to ocean water, we find

that the necessary length is about 443 meters for each treatment pipe. We also note that the total volume V of the treatment bundle,

$$V = \pi \left(\frac{d}{2} \right)^2 l M \ , \qquad \text{(Eq. 4.1.3)}$$

is much larger than the volume of brine output by the desalination plant for these values. If desired, d can be optimized so that V more closely matches W, assuming it is cost-advantageous to do so. V can even be somewhat lower than W assuming the processing rate of the treatment is smaller than the output rate of the plant.

4.2 Limitation with prior work

From this theory it is possible to see the difficulty of ion polarization using anything but a very long processing path. For instance, a previously-mentioned work [6] suggested using the Lorentz force to do this, however with a fairly short processing path. We can compute the necessary magnetic field strength to accomplish near complete ion separation on the solution flow through a 2.5 cm diameter pipe, over a length of 5 cm, which is a functional distance for applying a magnetic field of about 1 Tesla, for instance from a superconducting magnet. If we attempt to fully polarize the ions using an electromagnet with 100 current-carrying turns of wires, at 12 volts we would need to supply about 8 GW of power, which is approximately all of the electrical output from the Kashiwazaki-Kariwa Power Plant in Japan, the world's largest nuclear power plant. In contrast, separating the ions over a long distance of pipe using laminar flow requires less than 200 watts, about the power output of a typical solar panel in full sunlight.

4.3 Packing geometry optimization

There are methods of optimizing the efficiency of this process, since the magnetic field from each current loop extends beyond each pipe. An inefficient pipe packing would allow the magnetic field from one pipe to add destructively to the B-field of a neighboring pipe. Similarly, an efficiency packing arrangement would allow the magnetic field from one pipe to add constructively to the magnetic field of a neighboring pipe.

Consider a simple example. For two pipes with current directions shown; the effective magnetic field in (Figure 4.3.1a) is

$$B = \frac{\mu I}{2\pi r}(2.667), \qquad \text{(Eq. 4.3.1)}$$

while for (Figure 4.3.1b) a square array of four pipes, the effective B-field at the center of each pipe is

$$B = \frac{\mu I}{2\pi r}(3.046). \qquad \text{(Eq. 4.3.2)}$$

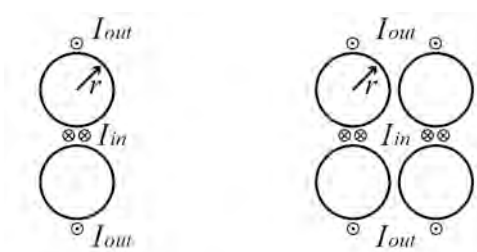

Figure 4.3.1a Figure 4.3.1b

Arrangement of pipes to increase B-field

The magnetic field strength increases significantly with advantageous packing of pipes, which should allow for significantly shorter pipe runs.

4.4 Processing time

The time that the solution needs to run through each pipe is the same as through the bundle, assuming a recirculating race is not used. This is provided by considering the kinematics of the flow through the pipe. Thus using (Eq. 4.1.2) the time t in the pipe is given by

$$t = \frac{l}{v_y} = \frac{lA}{f} = l\frac{\pi d^2}{4f} = \frac{1}{M}\frac{\pi d^2}{4f}\left[\frac{72\eta R}{q\mu IN}\frac{W^2}{d^2}\right]^{1/3}. \qquad \text{(Eq. 4.4.1)}$$

The most likely desired operation will be to increase the flow so that time t is minimized, however the fluid's speed should not be increased beyond laminar flow. Laminar flow is critical with this technique in order to minimize mixing of ion concentration streams, and it is likely that nearly seamless pipes may be required to keep as much turbulence from the flow as possible, perhaps even staging the processing to short treatment runs.

We will determine the flow f of the solution using the Reynolds number S of the system [9], which for a pipe is based on the pipe diameter d, the solution mass density ρ, the solution dynamic viscosity η, and the fluid velocity v_y,

$$S = \frac{\rho v_y d}{\eta} = \frac{4\rho f}{\pi \eta d}. \qquad \text{(Eq. 4.4.2)}$$

Solving for f in terms of S and inserting into our time equation we find,

$$t = \frac{\rho d}{MS\eta}\left[\frac{72\eta R}{q\mu IN}\frac{W^2}{d^2}\right]^{1/3}. \qquad \text{(Eq. 4.4.3)}$$

In order to achieve Laminar flow, we need to insure that S remains below a value of 2,320. This produces a very low fluid flow through the pipe, so processing (movement of

a volume of water through the length of the pipe) will take a large part of the day. Using a saltwater density of $\rho = 1{,}041\ \mathrm{kg \cdot m^{-3}}$ for 60,000 PPM seawater at a temperature of 25°C, $S = 2{,}320$, a pipe diameter $d = 10\ \mathrm{cm}$, and the other values as before, we find that $t \simeq 10\ \mathrm{hours}$. In order to stay laminar the water moves through the pipe at approximately the speed of a large garden snail of about 1 cm/s. Again, this time is less than the time required to create the volume of distillate *M*, which is a volume per 24-hour period. This is a rough estimate and it may be necessary to chill the treated water to slightly above freezing to minimize thermal agitation of the ions. If chilled (which comes at the cost of additional power), the mass density and the dynamic viscosity of the seawater would go up slightly, which would slightly increase the processing time of the solution in the pipe.

4.5 Working approximations and optimization considerations

Our length and time equations can be numerically approximated as follows:

$$l = \frac{1}{M}\left[\frac{72\eta R}{q\mu IN}\,\frac{W^2}{d^2}\right]^{1/3} \simeq \frac{37342}{M}\left[\frac{W^2}{d^2 IN}\right]^{1/3}, \qquad \text{(Eq. 4.5.1)}$$

$$t = \frac{\rho d}{MS\eta}\left[\frac{72\eta R}{q\mu IN}\,\frac{W^2}{d^2}\right]^{1/3} \simeq 1.55\times 10^7\,\frac{d}{M}\left[\frac{W^2}{d^2 IN}\right]^{1/3}. \qquad \text{(Eq. 4.5.2)}$$

As we see from these relationships, both the necessary treatment length and time are dependent on $W^{2/3}$. This suggests that the process will becomes increasingly efficient in terms of materials and operating cost as the output of the desalination plant *W* increases. Similarly, the length depends on $d^{-2/3}$ so a wider pipe would shorten the treatment distance. However, the treatment time is dependent on $d^{1/3}$, which is a less critical relationship than treatment length's dependence of d. So the choice of pipe diameter is

mostly a consideration of cost and construction of the necessary pipe lengths and bundle, rather than processing time.

CHAPTER 5

LFIP LABORATORY TESTING AND DATA

We tested this setup in a configuration as described previously. In our case, our magnetic field windings restricted us to a peak current of 1.5 amps. We recorded changes in potential difference across the section of 2.54 cm diameter PVC pipe in three locations, the collection end, the feed end and the center using 60,000 PPT Total Dissolved Solid (TDS) solution, made from distilled water and NaCl. A current was supplied to a longitudinally-wrapped coil of insulated 0.8 mm conductor diameter with a resistance rating of 10.15 ohms per 304 meters (20 gauge), with 24 loops of two strands to total 48 loops of total length 152 meters x 2. This created the transverse-to-flow magnetic field described earlier. Current to the coil was varied between 0 and 1.5 amps and was supplied from an 18-volt regulated Mastech power supply. Solution flow was provided by a submersible pump, which supplied 0.05 liters per second of flow. This was modulated from 'high' (0.05 liters per second) to low (~0.02 liters per second) to off, with no flow. Concentrate was returned to the source for recirculation with conventional PVC pipe. Additionally, for the purposes of identifying the response of the measurement probes alone, the pipe could be drained of solution. Potential difference was measured from stainless steel probes affixed to the pipe at three locations, and the voltage was monitored through independent Fluke digital multimeters. A giant magnetoresistance (GMR) probe was used to measure the strength of the magnetic field in the solution channel and it was consistent with our formulation given number of wire loops, supplied current and pipe diameter. The data are given in Table 5.1.

Table 5.1 LFIP experimental data

Trial	current direction	flow	current - amps	#1 - volts	#2 - volts	#3 – volts	#1 - change V	#2 - change V	#3 - change V
1	cc	dry	-	0.000	-0.001	0.000			
2	cc	dry	1.50	0.624	0.000	0.324	0.624	0.000	0.324
3	cc	high	1.50	0.929	-1.010	0.323	0.305	-1.010	-0.001
4	cc	low	1.50	-	-1.000	0.330		0.010	0.007
5	cc	high	1.50	-	-1.024	0.326		-0.024	-0.004
6	c	high	1.50	-	0.205	-0.313		1.229	-0.639
7	c	off	1.50	-0.868	0.200	-0.309		-0.005	0.004
8	cc	off	1.50	0.322	-0.914	0.313	1.190	-1.114	0.622
9	cc	high	1.50	0.295	-0.980	0.306	-0.027	-0.066	-0.007
10	c	high	1.50	-	0.244	-0.314		1.224	-0.620
11	-	off	-	-0.301	-0.360	0.000		-0.604	0.314
12	c	high	1.50	-0.859	0.275	-0.314	-0.558	0.635	-0.314
13	c	high	2.50	-1.116	0.380	-0.517	-0.257	0.105	-0.203
14	c	low	2.50	-1.134	0.392	-0.520	-0.018	0.012	-0.003
15	cc	high	2.50	-	-1.262	0.528		-1.654	1.048
16	cc	high	2.00	0.388	-1.140	0.424		0.122	-0.104
17	c	high	2.00	-0.933	0.310	-0.427	-1.321	1.450	-0.851
18	-	off	2.50	-1.085	0.391	-0.517	-0.152	0.081	-0.090
19	c	off	2.50	0.330	-1.233	0.525	1.415	-1.624	1.042
20	c	off	1.50	0.510	-0.964	0.316	0.180	0.269	-0.209
21	c	high	1.50	0.412	-0.935	0.314	-0.098	0.029	-0.002
22	c	high	0.01	-0.185	-0.265	0.001	-0.597	0.670	-0.313
23	c	high	0.25	-0.089	-0.353	0.051	0.096	-0.088	0.050
24	c	high	0.50	0.010	-0.460	0.104	0.099	-0.107	0.053
25	c	high	0.75	0.126	-0.530	0.156	0.116	-0.070	0.052
26	c	high	1.00	0.249	-0.587	0.206	0.123	-0.057	0.050
27	c	high	1.25	0.275	-0.767	0.262	0.026	-0.180	0.056
28	c	high	1.50	0.302	-0.910	0.313	0.027	-0.143	0.051
29	c	high	1.75	0.330	-0.999	0.365	0.028	-0.089	0.052
30	c	high	2.00	0.350	-1.083	0.417	0.020	-0.084	0.052
31	c	high	2.25	0.335	-1.154	0.469	-0.015	-0.071	0.052
32	c	high	2.50	0.349	-1.204	0.522	0.014	-0.050	0.053
33	cc	high	0.01	-0.475	-0.435	-0.001	-0.824	0.769	-0.523
34	cc	high	0.25	-0.482	-0.254	-0.051	-0.007	0.181	-0.050
35	cc	high	0.50	-0.180	-0.075	-0.108	0.302	0.179	-0.057
36	cc	high	0.75	-0.554	0.089	-0.161	-0.374	0.164	-0.053
37	cc	high	1.00	-0.659	0.169	-0.214	-0.105	0.080	-0.053
38	cc	high	1.25	-0.807	0.206	-0.268	-0.148	0.037	-0.054
39	cc	high	1.50	-0.922	0.255	-0.322	-0.115	0.049	-0.054
40	cc	high	1.75	-1.008	0.300	-0.377	-0.086	0.045	-0.055
41	cc	high	2.00	-1.070	0.320	-0.428	-0.062	0.020	-0.051

Trial	current direction	flow	current - amps	#1 - volts	#2 - volts	#3 – volts	#1 - change V	#2 - change V	#3 - change V
42	cc	high	2.25	-1.119	0.340	-0.480	-0.049	0.020	-0.052
43	cc	high	2.50	-1.154	0.366	-0.536	-0.035	0.026	-0.056
44	cc	high	2.75	-1.181	0.386	-0.588	-0.027	0.020	-0.052
45	-	-	-	-0.048	0.480	0.000	1.133	0.094	0.588
46	c	low	0.01	0.002	-0.239	0.001	0.050	-0.719	0.001
47	c	low	0.25	0.149	-0.383	0.068	0.147	-0.144	0.067
48	c	low	0.50	0.298	-0.508	0.137	0.149	-0.125	0.069
49	c	low	0.75	0.429	-0.615	0.205	0.131	-0.107	0.068
50	c	low	1.00	0.601	-0.675	0.272	0.172	-0.060	0.067
51	c	low	1.25	0.742	-0.775	0.335	0.141	-0.100	0.063
52	c	low	1.50	0.886	-0.945	0.406	0.144	-0.170	0.071
53	c	low	1.75	1.045	-1.056	0.493	0.159	-0.111	0.087
54	c	low	2.00	1.197	-1.137	0.580	0.152	-0.081	0.087
55	c	low	2.25	1.347	-1.195	0.657	0.150	-0.058	0.077
56	c	low	2.50	1.071	-1.254	0.758	-0.276	-0.059	0.101
57	c	low	2.75	0.971	-1.286	0.768	-0.100	-0.032	0.010
58	cc	low	0.01	-0.002	-0.304	-0.001	-0.973	0.982	-0.769
59	cc	low	0.25	-0.146	-0.175	-0.075	-0.144	0.129	-0.074
60	cc	low	0.50	-0.285	-0.041	-0.148	-0.139	0.134	-0.073
61	cc	low	0.75	-0.431	0.123	-0.229	-0.146	0.164	-0.081
62	cc	low	1.00	-0.588	0.178	-0.305	-0.157	0.055	-0.076
63	cc	low	1.25	-0.746	0.215	-0.383	-0.158	0.037	-0.078
64	cc	low	1.50	-0.908	0.243	-0.471	-0.162	0.028	-0.088
65	cc	low	1.75	-1.057	0.282	-0.552	-0.149	0.039	-0.081
66	cc	low	2.00	-1.230	0.317	-0.629	-0.173	0.035	-0.077
67	cc	low	2.25	-1.375	0.334	-0.712	-0.145	0.017	-0.083
68	cc	low	2.50	-1.521	0.352	-0.805	-0.146	0.018	-0.093
69	cc	low	2.75	-1.599	0.359	-0.840	-0.078	0.007	-0.035
70	cc	low	1.00	-0.604	0.129	-0.304	0.995	-0.230	0.536
71	cc	low	2.00	-1.200	0.370	-0.599	-0.596	0.241	-0.295
72	cc	very low	0.50	-0.304	-0.264	-0.146	0.896	-0.634	0.453
73	cc	very low	1.00	-0.601	0.120	-0.287	-0.297	0.384	-0.141
74	cc	very low	1.75	-1.065	0.360	-0.515	-0.464	0.240	-0.228
75	cc	very low	2.00	-1.228	0.352	-0.592	-0.163	-0.008	-0.077
76	cc	very low	0.50	-0.347	0.293	-0.143	0.881	-0.059	0.449
77	c	very low	0.50	0.286	-0.735	0.136	0.633	-1.028	0.279
78	c	very low	1.00	0.584	-0.907	0.274	0.298	-0.172	0.138
79	c	very low	1.50	0.890	-1.000	0.411	0.306	-0.093	0.137
80	c	very low	2.00	1.182	-1.142	0.547	0.292	-0.142	0.136
81	c	very low	2.50	1.401	-1.237	0.654	0.219	-0.095	0.107
82	c	very low	0.25	0.143	-0.583	0.060	-1.258	0.654	-0.594
83	c	very low	1.50	0.887	-0.948	0.382	0.744	-0.365	0.322

CHAPTER 6

LFIP DATA ANALYSIS

If we look at our flow tube as a battery, where the ion polarization produces a change in voltage across each set of test electrodes (which are placed across the cross section of the pipe in three locations) then we see that the combination of flow and current produces a measurable voltage change. Our theory predicts that the slower flow will produce a more laminar flow and thus we should be able to see more consistent polarization with low flow than with high flow. Our tests confirm this, as trials 46 – 83 show a correlation with current direction (and thus direction of magnetic field) and probe voltage, where clockwise currents produce consistent positive voltages at probes #1 and #3, and consistent negative voltages at probe #2. (This opposite sign is likely explained by the polarity of the meter as connected to the probes, but we didn't notice this trend until after we took the data.) Conversely, counterclockwise current produces the opposite effect in these same probes. The clockwise currents produce a magnetic field directed downward through the tube, and with the flow going to the left, this should push the ions left or right (transverse to solution flow) depending on the charge of the ion. The opposite effect will be found with the counterclockwise charge current. The other trials also show a smaller correlation, possibly due to the increased turbulence of the higher flow. It was also noted that the probe voltages increase with increased magnetic field, also consistent with the theory, due to higher polarization.

A very important facet of these findings is that the probe voltages can also pick up polarization effects that are not necessarily consistent with a brine-treatment operation, such as reorientation of anisotropic molecules in the solution. To isolate this effect we took measurements with zero flow, which should theoretically produce no Lorentz force polarization effect. These corrections are shown in trials 7, 8, 11, 18 – 20.

As seen in Figure 6.1, the probe potential increases at the far probe with increasing magnetic field current. This correlates with increased ion polarization due to increased time spent in the magnetic field. (In the next phase of the experiment we hope to measure our ion polarization in a way that allows us to correlate the experiment to our theory. For this trial though, the increased probe voltage as an indicator of polarization is the test we can verify with our relatively short pipe.)

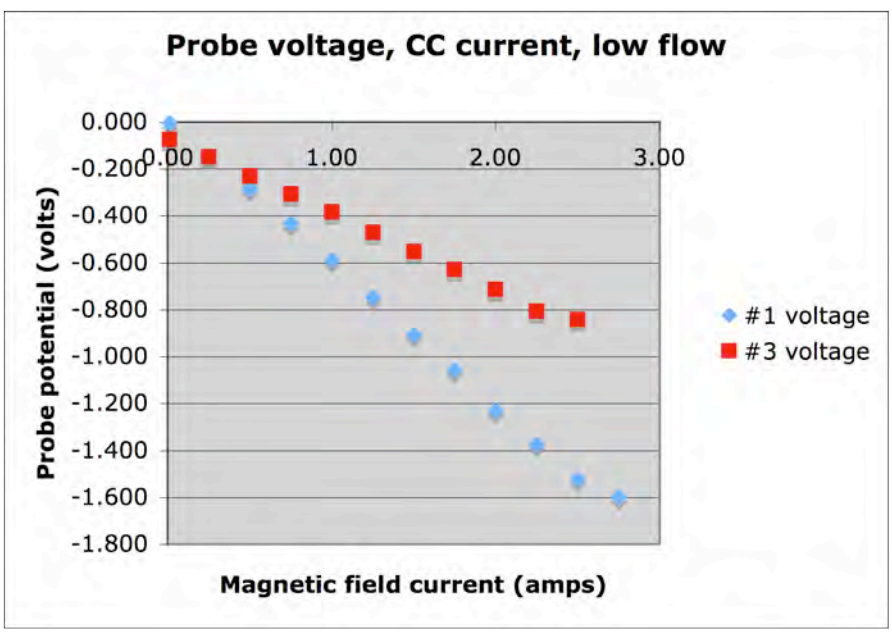

Figure 6.1 Probe voltage versus B-field current with counter-clockwise current

CHAPTER 7

LFIP CONCLUSIONS AND FUTURE WORK

We believe we have a good start on the theory, but the experimentation phase of this work has barely begun, and considerable work remains for us and other researchers. Specifically, a concrete theoretical connection is needed to connect the probe voltage as a function of the ion-polarization and the Lorentz force as a function of magnetic field and flow. Since these differences are fairly small on the short length scale, the best hope to make this connection is by analyzing several sets of trials, identify the noise inherent to the setup and then identify just the Lorentz-force induced polarization. More theoretical work is needed as to the effects of reorienting molecules (due to anisotropy) in the solution without necessarily moving them through the solution. This is necessary to isolate these effects from the desired effect of ion migration.

The biggest question related to this research is if the desired ion polarization can overcome any small effects of turbulence due to surface roughness of the pipes even if the flow through the pipe is laminar. Given the necessary processing length, a seamless pipe treatment system may need to be developed and the interior walls of the pipe may need to be treated with a low-friction material. This will be difficult and expensive for long straight pipes, but may be possible with recirculating races. Of course, recirculation adds to the question of turbulence as the fluid changes direction to round corners. Another issue will be random thermal agitations through the brine, which may give rise to a random movement to the ions offsetting some of the polarization effect. Cooling the

brine to reduce this contribution may help, and additional theory may be required to possibly find an optimum temperature for reduction of thermal motional and optimization of diffusion, density, and mean free path of the hydration spheres across the flow. Further theoretical examination may be required to examine possible stabilizing effects of the velocity gradient across the flow.

It should be possible to build a unit to test this possible ion polarization even without understanding all the ramifications of all these contributing effects, possibly by creating an error factor that folds these contributions into an empirically derived constant.

The potential reward is significant, and there may be an opportunity to use basic physics to contribute to the solution of a real-life developing environmental problem. The alternatives solutions in this area are few, and if this method is possible, the current theory indicates that using this method may lead to an energy and cost-effective solution.

A surprising part of this research was perhaps the theoretical dependence on the treatment length. The theoretical efficiencies of this system only begin to emerge strongly when a lot of water is treated over a long distance. We hope to be able to support this theory with eventual tests.

The most important remaining area for the theory of this research is to consider the significant effect of the increased B-field due to advantageous packing of the pipes. As we have seen from (Eq. 4.3.2) the effective B-field rises rapidly with clusters of pipes which should significantly lower the length requirements of this process and even make the process feasible for an industrial scale.

SECTION II

CHAPTER 8

PERSONAL-SCALE PASSIVE SOLAR DESALINATION (PSPSD)

8.1 Scope

As the world's population grows and water sources are depleted and contaminated, desalination is increasingly becoming an important tool to satisfy human, industrial and agricultural demands for fresh water. Currently, less than 1% of the world's water is supplied through desalination, but this is expected to increase, as the desalination industry is projected to grow by 9.5% per year over the next decade [10]. The most common methods of desalination are driven by electricity or hydrocarbon fuel, but the use of direct solar thermal energy to desalinate water was used in 1872 in Chile, in a 50,000 square foot solar distillation array to provide water for mules in a mining operation. The first widely used personal-scale solar stills were used during WWII, as inflatable units to provide emergency water on life rafts [11]. While several solar desalination methods exist, the simplest and most common is the passive solar still (PSS). With this method, the sun is used to heat a greenhouse-like structure containing saltwater or contaminated water, the feed water is vaporized, it condenses inside the device on the condensing surfaces, and it is collected and then removed from the system. In this sense, the PSS is the system that most closely resembles the Earth's own rain-making process, except that in the atmosphere, water vapor condenses on seed nuclei rather than the condensing surfaces of the PSS.

The main focus of this research is to examine this process and suggest potential improvements to the desalination efficiency of the PSS. The PSS is an important segment of research in solar desalination since this device can be simply constructed, and is ideal for low-cost applications in Developing Nations.

8.2 Outline of water problems and applications

Nearly one fourth of all people on Earth suffer from inadequate freshwater supply [12]. Population on Earth continues to increase while sources of ground water remain stable at best, and often decrease due to overuse and contamination. People in Developing Nations face increased strain on their existing water supplies since their populations are growing faster than those of many industrialized nations. Between 1900 and 1995, the demand for drinking water grew twice as fast as the world population, and by 2025 researchers suggest that this demand will grow by an additional 40%. Further, by 2050, some forty countries could lack drinking water [13]. This deficiency will impinge upon development and health of people in developing nations. At least 80% of the world's inhabitants live in arid and semi-arid countries, and among those, 40% are currently suffering from drought and at least half a billion people in developing countries suffer from water-borne illnesses [14].

Many people in developing nations are forced to use water from contaminated sources, which can lead to serious damage to health. Available water shrinks per capita because population grows [15]. These health dangers include diarrhea, cholera and other water-borne illnesses. Combined, the World Health Organization reports that water-borne illnesses kill more people each year than war. While many of these diseases need not be

fatal and can be easily treated in industrialized nations, lack of medical infrastructure and lack of access to clean water renders these diseases more deadly than they would normally be in a healthy populace. Further, lack of coordinated rain water collection leads to water pools on flat roofs and in villages which produce breeding areas for malarial vectors.

Not only is population increasing, but increased industrialization in all countries, rising living standards in developing nations, and expansion of irrigation agriculture has led to increased strain on existing water supplies [16]. Countries in the Middle East and North Africa region experience the most severe water shortages. Increasing industrial and agricultural activities also contribute to the depletion and pollution of freshwater sources [17].

8.3 Water distribution and need

On Earth, 96.5% of the water is saline. Of the remaining 3.5% freshwater, about half is available for use, the rest is in polar and glacial ice [18]. This leaves primarily groundwater, and water from lakes and rivers. More than half of the ground water available for use is saline, and this percentage rises as freshwater is removed from the ground near salt and brackish water sources, which forces saltwater intrusions into wells which then renders them useless without desalination. One study by Bouchekima [13], claims "hundreds of millions of women and children are enslaved to the daily water quest." This refers to the common practice in Developing Nations of having to walk several miles to water sources. Bouchekima further states that water shortages reduce a population to "destitution and poverty". He continues, "By the end, this population has no

choice but disappearance or exodus." It would seem that access to clean water differentiates many people in Developing Nations into a state of living that has no resemblance to what we would consider 'modern.' Another study [19] states that modern agriculture "swallows considerable amounts of good water" to produce increasing amounts of food necessary to meet growing populations. It is important to consider the fact that increasing populations not only require an additional few liters per capita per day of drinking water, but they also require many times more freshwater to produce their food requirements than people in Developing Nations.

One study from 1982 from the World Bank [14] found that of the then 2.4 billion people living in developing countries, less than 500 million of them had enough clean potable water. It also found that each year, an additional 70 million people lack potable water. More recent data from 2006 [20] shows that waterborne diseases have caused an estimated 1.8 million deaths each year and 1.1 billion people lack potable drinking water. Comparing these data indicates that a higher percentage of people in Developing Nations have gained access to clean water — likely the result of well water projects — but comparing this recent data with Kumar and Bai [4] indicates that the percentage of people who suffer from water-borne diseases is increasing.

8.4 Introduction to freshwater replacement

There are three potential solutions for these increasing problems: use less water, capture freshwater that was previously lost to the ground, atmosphere or ocean, or produce water from previously unused sources. It is the last option that is the primary research goal of this work. While considerable research has already been done on

desalination, this research focuses on a small area of desalination, specifically personal-scale, solar-powered, passive desalination.

Research in desalination grows with the industry. There are currently more than 15,000 desalination plants in more than 120 countries and it is estimated that this will grow by 100% between now and 2015 [14]. This number shows a mix of various desalination technologies, but primarily either reverse osmosis systems or multi-effect distillation systems. These two methods are fundamentally different, in that osmosis uses molecular screens to separate low-concentration salt water from high-concentration water, while distillation removes pure water a molecule at a time as vapor and re-condenses it. Reverse osmosis typically has the edge in efficiency, but distillation is a far older and simpler method and is more popular in countries that have less access to complex components such as energy-recovery systems, molecular screens and prefilters. A negligible component of desalination is solar, due to relatively low efficiency at scales comparable to typical large desalination systems that produce more than 50,000 liters of water per day. Nearly 60% of the world's desalination capacity is currently in the Arabian Gulf countries [21]. This abundance of desalination capacity may be partly explained by both the clear need for potable water in this arid climate and also the relatively high national wealth to afford these technologies.

While solar desalination currently accounts for a relatively insignificant portion of the world's desalinated water, high solar radiant flux is usually coincident in areas of the world that need water most [22]. The opportunity to use solar power to desalinate water in good locations is considerable. In remote locations, engineering expertise, spare parts, fuel and electricity are often difficult to source. Solar desalination can provide water

obtained simply, and using only direct energy from the sun, these logistical problems can be avoided.

Exploiting renewable resources can reduce the energy requirements of conventional desalination. This is because areas where water is needed are most often recipients of ample solar energy. Most developing countries with vast areas but limited infrastructure seem well experienced in the application of solar energy [17]. The basic feasibility behind solar water desalination is further established when one considers that our natural water supply comes from the largest simple desalination system in the world [21], nature's own water cycle.

Thus the simple solar still has been proven in theory long before we had the material to exploit the process on the small scale. Other names for this system include [11]: greenhouse still, roof-type still, simple still, basin-type still, and conventional-type still. Our own research in this area has contributed to a technology transfer project with the market-name SEA Panel, where SEA is an acronym for Solar Evaporation Array, along with three U.S. Patents.

CHAPTER 9

PSPSD BACKGROUND AND PRIOR WORK

The primary motivation behind this portion of research is to develop a solar still technology that is inexpensive and quick to set up for use in Developing Nations and in disaster recovery.

9.1 Classification of solar stills

The most common solar basin type is the passive basin-type still, which forms the majority of the world's installed solar still capacity [23]. This is the simplest type of solar still, essentially comprising just a basin that holds the raw water, and a transparent surface which both allows solar radiance to pass through and warm the interior of the still and the raw water and then allow the evaporate to condense on the inner surface of the transparent barrier, after which the condensate runs along this surface and drips into a collection channel. This configuration has some significant deficiencies compared to *active* systems, mainly that the surface to which the evaporate condenses is at a relatively high temperature due to also being the surface through which the solar radiance passes. The thermodynamic efficiency is increased in non-basin configurations where a separate condensing surface is used, but the overwhelming advantage of the basin still is its simplicity. In the words of Löf [24] "there is no moving equipment, there are no high or low pressures in the system, and the plant is substantially self-operating." They are considered one of the cheapest solutions for purifying saline or brackish water [25].

As a further classification of passive solar stills, the simplest and most popular is the single basin, single slope still (SBSS). For our tests, the rigid thermoformed stills were considered double-slope, single-basin, (DSSB) with each unit consisting of three DSSB units connected at the front and sharing common distillate collection channels. The flexible polyethylene units were single-slope, single-basin. While DSSB designs do well in the summer and in the tropics, SBSS provides higher yield in winter and at higher latitudes [26]. One study found that for locations with latitude higher than 20°, the single slope still is preferable [27]. Typical desalination methods are shown in Table 9.1.1, assembled from [16].

Table 9.1.1 Classification of desalination methods

A. Processes that separate water from the solution

1. Distillation or evaporation
    a. Multiple-effect long-tube vertical
    b. Multistage flash
    c. Vapor compression
    d. Humidification (solar distillation)
2. Crystallization or freezing
    a. Direct freezing
    b. Indirect freezing
    c. Hydrates
3. Reverse osmosis
4. Solvent extraction

B. Processes that separate salt from the solution

1. Electrodialysis
2. Osmionisis
3. Adsorption
4. Liquid extraction
5. Ion exchange
6. Controlled diffusion
7. Biological systems

Gilam and McCoy [16] state that since salt in water is usually 3.5% or less of the total mass, that the processes in category B (salt removal) would "appear to have a theoretical advantage" over those in category A (water removal). They further note, however, that in present systems, no over-all advantage is obtained. While the authors of this paper did not note any specific advantage, we note that in 2009, the vast majority of commercial desalination systems are either reverse osmosis or distillation/evaporation systems. Also, in contrast to reverse osmosis, the efficiency of solar desalination is not closely related to the salinity of the feed water [23].

The economics of these various desalination methods will not be examined except as they relate to the subject of this research, solar distillation. While the economics are not key to this research, it is worthwhile to consider them, in order to properly establish the applications and constraints of the technology. In 2005, the overall desalination industry produced about $25 \times 10^6 \ \mathrm{m^3/d}$, and is roughly evenly divided between distillation and reverse osmosis processes [28]. Since that time, efficiency increases and decreasing prices of reverse osmosis has led to an increasing share of reverse osmosis in the desalination industry. As mentioned earlier, solar desalination's share of this total volume is currently insignificant.

Desalted water is an expensive product relative to conventionally-obtained freshwater, but solar desalination has the unique opportunity to be useful far from established electrical and engineering infrastructures. In some regions, it was found that solar stills farther than 80 km from freshwater sources produced water for a lower price than trucking in potable water [19]. Similarly, water brought in by tanker for island communities is often more expensive than on-site desalination. The cost of transporting

water long distances by pipeline also incurs a cost for pumping, maintenance and installation, and the authors find that for relatively small water needs of less than about 40 m^3/day, solar distillation could supply water for about half the cost of a pipeline.

Of the established desalination methods, it was found that solar-driven reverse osmosis has the highest efficiency of all the tested methods [29], while solar stills are claimed to be the least flexible method of solar desalination (due to absolute dependency on solar radiance) with high costs [21]. These two conclusions come from different authors, and in fact solar-driven reverse osmosis is also dependent on solar radiance. Reverse osmosis systems are pump-driven, and always have initial current draws higher than their running current. This would require some method of energy storage for starting the system, and it also restricts the system to be used during peak solar radiance. Water can be stored, and if the ability to tie the photovoltaics to an electric grid is available, then the solar panels can be used to feed power back into the electrical grid, and then when the desalinated water is needed, it can be powered directly off the grid. This would allow a smaller photovoltaic array than would be necessary if it were used to directly power the reverse osmosis pumps. Similarly, while the restrictions of solar desalination are obvious, many solar desalination systems can also be used to capture rain, which extends their capability in overcast weather and rainy seasons. Considering these factors, studies have concluded that solar desalination may be the best solution for remote areas and small communities where potable water would otherwise not be available [19].

Arid lands in particular have been concluded to offer great potential for solar desalination [30]. This is likely due to the high solar radiance in these areas. While areas with lower relative humidity have no effect on the solar desalination process (since the

interior of the units is always at 100% relative humidity) dryer air allows for higher solar radiant flux. The average daily radiation in arid lands exceeds 5000 Kcal/m^2. This leads to an annual rate of about 30×10^{15} kWh, which is more than six times the world's oil reserves, where 1 MWh can be produced from 0.112 barrel of oil [21].

While there is a large amount of solar energy incident on the ground, coupling that energy to useful desalination processes is not easy, in fact, the maximum Carnot efficiency of a well-insulated solar still is abut 8%, and usually closer to 6%. A principal focus of this study is to examine existing productivity rates and methods to raise productivity. Even state-of-the-art, large-scale solar desalination systems have "relatively low productivity rates [17]". This requires much more land-area per unit of water output than conventional desalination methods, thus once water requirements rise above approximately 50 m^3/day, it usually makes more sense to use conventional reverse osmosis or distillation plants. This rule-of-thumb principally assumes the established productivity of single-basin, passive solar stills. While this is the only widely installed type of solar desalination system, more advanced solar desalination systems will presumably raise this limit due to their higher efficiencies. However the clear advantage of solar desalination is that operation costs are considerably lower than conventional electric and oil-driven processes, and thus have applicability in remote areas and areas where conventional energy is scarce. (In the case of personal-scale desalination, the operating costs can be considered close to zero, because the user performs maintenance and operation.) Further, solar desalination is a sustainable method of water production and thus has environmental benefits over conventional methods.

Assuming the range of applicability is considered, solar desalination has the capacity for dependability and cost competitive with other processes [23]. Further, fuel prices cannot only be expected to rise throughout the world (which makes solar processes more attractive), but fuel prices for isolated and remote communities are already more expensive due to transportation. It has been reported that solar distillation could be the most favorable method of potable water production for tropical areas without the necessary infrastructure to support more complex methods [31]. Further, the simplicity of solar desalination (since it has few or no moving parts) offers an economic advantage over methods that require extensive maintenance and operating costs [19]. One such application may be coral islands (due to the scattered habitation on the islands) as a supplement to rainfall collection [32], and also because such systems have a small environmental impact [31], assuming their brine output is managed.

Currently, the world's share of renewable energy used for desalination is only 0.02% of the total renewable energy used [14]. This will undoubtedly rise as desalination becomes more prevalent since a principal use for desalinated water is in locations where renewable energy often offers a cost advantage over conventional energy. Of course, renewable energy has yet to gain a significant market hold, and aside from hydroelectric power, renewable energy sources (including solar, wind and geothermal) produce about 1% of the world's energy [17]. While this low figure could be taken as a relative failure of renewable energy, this statistic hides the wide success of hydroelectric, which accounts for about 16% of the world's total energy production, and above 50% in some areas of the world. Most of this growth has appeared since WWII. If hydroelectric power is a demonstration of the world's acceptance of simple renewable power, then the future of

solar, wind, wave, tidal and geothermal could be significant. Energy and water will likely be more related in the future, since it is clear that desalination (an energy-intensive operation) will play a critical role in future water supply.

Small-scale systems have a clearly defined niche in water production; they produce from 1 – 6 liters per day, enough drinking water for an individual or a family [33]. Slightly larger systems can provide water for a neighborhood or village. One of the benefits of solar stills is that they can be constructed, operated and maintained by local people and without significant expert and highly trained labor [31]. These advantages can be further extended for so-called "personal-scale" desalination in that systems can be operated and installed with no specialized training, and simple included pictorial instructions should be sufficient for operation.

Unlike conventional reverse osmosis and distillation installations, solar desalination often lends itself to using local materials and local labor, and installation accounts for about 35% of the total cost of the still per unit area [13]. The simple solar still is the only solar desalination method to have any kind of widespread, non-experimental use, and it is the oldest method of solar desalination so that design improvements have been made to increase water output [13]. However, research in advanced forms of solar desalination is ongoing with tremendous advances in efficiency. These include hybrid systems, and solar collector systems where the hot water is collected apart from the desalination system, and then used for conventional thermal desalination processes [28]. In general, solar stills are considered a form of 'direct desalination' while any process that has an offline component or use solar-heating in the process is considered 'indirect desalination.'

9.2 Evaluation of systems

An established set of criteria exists for the evaluation of solar desalination systems when evaluating site requirements [11]. These requirements can be modified and extended for personal-scale solar desalination (PSSD).

a. Climate - Skies generally clear and with bright sun during the period necessary for potable water making. If water needs to be provided during a rainy season, then the system should include the ability to capture rain.
b. Scale of need - To supply water for an individual or family. Children typically require half the drinking water of adults. While PSSD is capable of collecting water in excess of 6 liters per unit, collected water will usually be used principally for drinking, cooking and simple washing. There will likely not be enough water produced for bathing, agriculture and extensive cleaning. If water is needed for a neighborhood or village then units should be arranged in some form of array to facilitate potable water making. This could be as simple as tubing, which allows for filling of units from a single source, and collection of distilled water to a single storage.
c. Site - Unobstructed solar radiation and close to salt or brine water sources because units are typically filled by hand.
d. Preliminary size - Water requirements per person vary, the low estimate is 2 liters per adult per day, but 3 liters is more accurate for most climates where desalination would be necessary. This does not include water used for

personal sanitation and washing, but these tasks can presumably be accomplished with nonpotable water.

e. Design - What size units and how many units are needed for the application. For example, a family with two parents, and three children under ten would need approximately 10 liters of potable water per day as a minimum requirement. Is the climate rainy enough to support included rain capture as a method to increase output of potable water?

f. Estimate of monthly yield - PSSD typically produces higher outputs in the summer than winter, and during the rainy season, most of the water 'produced' though the system will likely be captured rain. One standard rule of thumb for solar desalination systems is that each square meter of basin area will produce about 4 liters per m^2 in summer with steady sunlight in hot climates. This output will vary with different units, and will fall to less than half during low-sun months in higher latitudes.

g. Rainfall contribution - Some PSSD systems will support rain-capture, some will not. Storage of the rain needs to be considered, as does average site rainfall and required time of storage.

h. Monthly needs versus production - Winter months or rainy months will produce less distilled water. (However effective rain-capture can effectively outpace per-day output of distilled water.) Assuming relatively constant water needs through the year, low-output months will need to draw from excess production from the warmer months, and long-term water storage will be necessary. Can excess water be used for drip-irrigation?

i. Estimate of cost - PSSD's primary (and perhaps only) cost is initial purchase price, since solar distillation does not use filters or consumables and specialized labor and fuel are not necessary. Will arrays of PSSDs require someone to manage them? Does the purchase price of PSSD components allow for resale of water produced by local water merchants and entrepreneurs?

j. Other considerations - Is the unit easy to use, attractive, durable, resilient to weather and animals? Can it be operated so that contaminated water is solar pasteurized to prevent algae growth inside of the unit, or will the unit require biocide during cooler months?

9.3 The use of plastics as a replacement for conventional materials

Considerable work has been done in the last twenty years on improving the efficiency of the solar still by using multiple effects, separate collectors and condensers, and coupling with hybrid systems. Much of this work has been successful. Our work focuses on the simple basin still because the ease of repair and low cost allow for applications in Developing Nations. Several of our previous references point to the need for simplicity in remote locations and economically developing areas. Finally, this work focuses exclusively on transportable, stowable solar stills, which can be manufactured industrially, and then set up on location by the end-user. Löf mentions such a distiller developed in Algeria and Australia, made of asbestos cement for the tray, and glass for the cover, but mentions that they were no longer in production, at the time of publication [24]. Due to our requirement for transportability, construction of lightweight

plastic was the logical choice, in that it is inexpensive and weatherproof. However the use of plastics with solar stills has potential problems that need to be considered.

The most common material for conventional solar stills is glass for the condensation barrier and either cement, metal or fiber-reinforced materials for the basin. While glass is breakable, it has the advantage of being resistant to damage from ultraviolet solar radiation, as well as weathering that would otherwise damage roll polyethylene, Plexiglas or thermoformed plastic panels. Notable research has examined the potential of using plastic for solar stills [24]. This research concludes that the principal problems encountered with plastic are the "fragility and short service life" of the plastic material. This author concludes that expendable plastic solar stills "do not appear to have significant potential in the United States or other countries" for meeting water requirements due to "less-than-complete reliability." They also point out the lack of wetability of the transparent barrier which may lead to distilled water dripping back into the brine, wind damage to the plastic and overheating of black polyethylene basin bottoms where the basin liner may have a melting point exceeded in a dry distiller.

The concerns are valid, but our tests have shown that using roll polyethylene considerably thicker than what was used in earlier tests can mitigate many of these concerns. Specifically, for the clear barrier we used a 6 mil (0.1524 mm) thick clear plastic with added UV-inhibitors, which is manufacturer-guaranteed to have a useful service life exceeding four years. (Our current tests have seen no significant degradation going onto our first year of constant sun exposure and our units have held up in high winds.) We addressed problems of wetability by using notably steeper condensation barrier inclines over typical glass inclines, and in some cases by addition of a food-grade

anti-condensate coating on the inside of the clear plastic barrier. The problem with hot spots on the black basin material has been mitigated somewhat by using fiber-reinforced polyethylene which has a melting point about 10°C higher than unreinforced material. We believe that by addressing these concerns, polyethylene can offer advantages for our intended purpose.

Other researchers found that stills made of plastic had a significantly lower productivity rate due to fogging and dripping from the cover to the water feed channel [23] [27]. Other researchers examined different plastic stills [19] including inflated and a v-shaped design, and concluded that the "stability of these designs against weather conditions was not satisfactory." We found that the anti-condensate coating allows the distillate to sheet from the inside of the clear barrier, and we also found that approximately doubling the angle of inclination of the condensation barrier improved the draining of condensate off the inner clear surface. Other research has looked at the possibilities of using polyethylene or PVF/PVC (polyvinyl fluoride or polyvinyl chloride) [11]. One study looked at "family sized" units that produced about 20 liters of water per day [32]. The original design of these units used Tedlar (a roll plastic) for the cover, but the material was apparently not UV-resistant, and it failed in less than a year and had to be replaced with glass.

9.4 Adjustments to designs for plastic-compatible solar distillation

Typical angles of inclination are between 10° to 15° for glass condensation surfaces [34] with some slopes going as high as 32° [35]. Most typical inclinations are kept to a minimum to conserve materials and keep construction costs low. Since distillate

is less prone to sheet on untreated plastic, the inclination angle is typically increased, and in our case it was between 20° and 30° depending on configuration. The tilt angle has been shown to influence the overall efficiency of the still [14] but most typically, this effect is fairly small and one study showed that the slope of a glass cover between angles of 10° and 45° had no measurable effect on efficiency [32]. These plastic systems can be divided into three general types [24]:

1. Inflated or wire-supported all-plastic tubule condensing surface with enclosed salt-water tray,
2. Horizontal basin with separate plastic covers supported by framing,
3. Circular basin with upright or inverted plastic conical cover.

Our polyethylene test system shares some of these features, but it is made from very thick polyethylene, supported by ½-inch thick PVC tubing, so it can be considered a hybrid of types 1 and 2. Our thermoformed panels were self-supporting, and thus had a commonality with other researchers' test units made from polystyrene and Plexiglas [36].

One of the key considerations with our research is that recent advancements to roll polyethylene have been developed due to the expanding market in agriculture for plastic-covered greenhouses. It's reasonable to conclude that the roll polyethylenes have benefited from some of the same advancements in durability, performance, and lowered costs in the last ten years as many other petroleum products. Löf tested small solar distillers that had a commonality in desired deployment with ours. Löf states that the objective has been to use a design "employing cheap, portable materials which be easily erected in the field." Other researchers, including Phadatare et al. [22] and Hamed et al. [26] examined the use of simple solar stills with plastic construction. Additional research

by Porteous [23] notes that plastic offers a considerable advantage with the salt-water and marine environment in that significant problems with corrosion can be mitigated using components of plastic, rather than metallic, construction.

9.5 Background research on barrier cooling

Tiwari and Bapeshwara produced the basic theory behind using a thin film of water to lower the temperature of the condensation barrier to attempt to increase desalination efficiency [34]. The authors found that a "uniform flow" of water over the glass condensation barrier produced a "remarkable decrease" in the temperature of the glass cover. The daily distillate production was found to be nearly doubled with this method. They measured both the temperature of the glass cover and the temperature of the water film and found they were nearly in thermal equilibrium. The authors concluded that the water film speeds the condensation process and enhanced productivity. However they also found that an increase of water flow over the glass beyond a very thin film led to a *decrease* of distillate output.

One study [37] found that using a thin film of water to cool the condensation barrier seems to have shielded the still from the effects of wind speed. Normally, increased wind speed leads to slightly higher efficiency because the heat is removed more efficiently from the outside of the condensation barrier. The authors pointed out that this could be a useful feature, since the production rates would be stabilized in areas that receive sporadic wind. They also note that this water film will tend to self-clean the surface of the barrier, which is critical for dusty conditions since the incident radiation can be severely limited by dust and dirt on the barrier. In whole, these researchers found that careful barrier cooling can increase efficiency by up to 6 percent.

Also important to this same study is that the researchers used the cooling water as refill water for the still, and a component of this preheated water was used to replace water that evaporated from the feed basin. This is a similar setup to our own experiment and an important result for us.

While they did not use water to cool the barrier, the effect of cooling the condensation surface has been shown to produce increased efficiency [27]. Other methods mentioned in this work fit their condensing surfaces with air-cooling fins to achieve efficiency increases of between 30% and 70%. This research also uses a double glass layer rather than a single layer and passed cooling water between the glass layers to both capture the latent heat of condensation on the collection barrier to increase production efficiency by 20%.

Abu-Hijleh and Mousa [37] did a numeric model of barrier cooling with the single basin still and found that effective use of this method can increase the thermodynamic efficiency of the still by up to 20%.

9.6 Evaporation basin

In any solar still, the feed of the salt concentrate water is a concern. If new concentrate is added too quickly, the temperature of the evaporation basin falls and thermodynamic efficiency suffers. If the concentrate is held too long in the basin, output suffers because output decreases as solution salinity increases. The primary methods of feeding saline water to the evaporation basin is either continuously or with the batch system [38].

An important development in solar stills has been the development of the wicking basin. In this configuration, an absorbent wicking material draws the salt solution onto its fibers and dramatically increases the total surface area of the wetted surface over a simple basin filled with water. As a further advantage, the capillarity of the wicking material allows the evaporation basin to be inclined to the sun angle [39], which is obviously impossible with a conventional water-filled basin. Ayber et al. [33] found that use of a wicking material was able to increase productivity threefold. As the salinity of the water in the basin increases (for zero-brine configurations) the wicking material is squeezed-out and then removed to allow the unit to run dry, and the salt crystals removed from the basin. The wicking material is then replaced and the process starts with fresh water.

Considerable work has been done in other research on optimization of basin depths. Typically, the shallower the water, the more efficient the distillation since there is a smaller mass of water to heat and thus there is less thermal loss [24]. Tiwari and Madhuri found that an insulated basin at shallow depths produced twice as much distillate as a deeper basin [40]. Murugavel et al. concluded "when compared with other parameters, the basin water depth is the main parameter that effects the performance of the still [27]" . Varying conditions can alter this balance, because a well-insulated deep-basin still can essentially store daytime solar energy and continue to produce distillate well into the night as the basin cools. Even though the deeper basin takes longer to warm at dawn, it can take advantage of cool evening temperatures, which lower the temperature of the condensation barrier, and thus increases the total thermodynamic efficiency [41]. The connection between basin depth and output is a well-studied area. However, there are limitations to how much efficiency one can produce from modulating the basin depth for

personal-scale solar stills, since the simplicity of the device does not allow active depth monitoring and regulation, which is possible on large-scale systems. In personal systems, the user adds the raw water when necessary, and forcing the user to do this job too often will create hardship. Secondly, to take advantage of very shallow basin depths requires a carefully leveled basin surface, something that may be difficult with user installations.

Other researchers have examined ways of increasing solar still output by changing the characteristics of the basin itself. In its most simplistic form, a basin is simply a volume of water where the surface area is the source for the evaporate. By increasing the effective surface area of the basin, and by allowing it to absorb more light, it is possible to increase the effective output of the system. Murugavel et al. found that by adding black dye to the water that output production rate was increased by 29% [27]. These same researchers found that floating a perforated black aluminum plate in the still increased the still output by up to 40%. Another study found that adding wire sponges to the basin increased output [42]. These same researchers also found that they could significantly increase the output of their stills by adding locally sourced dark-colored stones to the basin, without the problems of the corrosion presented by the wire sponge. This is an important result for us, because dark rocks are available in most locations where such a personal still would be used. The stones were inferred to increase the output by increasing the effective surface area of the basin (since the water's capillarity drew it up the stones somewhat, and because the rocks added thermal mass to the basin). One other important result for our work was from Murgavel et al. [27] who found that sponge cubes added to the basin increased distillate production by up to 27%. Sponges are lightweight and thus can potentially be readily shipped with the units to their point of deployment.

Finally, Murugavel et al. [27] found that covering the basin with a layer of black cotton cloth increased output by acting as a wicking material and absorbing more light.

The workability with these methods needs to always be considered, since salt and minerals will deposit on the materials added to the basin and lower productivity. While it is fairly simple for a user to squeeze out wicking material and empty brine out of basin or collect crystallized salt, the addition of many stones can make it difficult for the user to clean the basin of salt or waste.

Additional research has been performed on the process of adding surfactants to feed water to lower the surface tension and thus presumably increase distillate output [43]. Typical surfactants used were sodium lauryl sulfate (SLS) and this produced modest output gains. We performed a trial using a surfactant of common dish soap in the feed water, but our results did not encourage further examination.

Another area of research is the insulation of basins. The essential issue is that basins need to be insulated from heat loss to maintain high distillation outputs. For testing, we compared uninsulated controls to panels with various types of thermal insulation.

The typical salt source is about 33,000 parts per million (PPM) of total dissolved solids (TDS). But inland seas often have salt contents as high as 43,000 PPM (i.e. Red Sea) or as low as 7,000 PPM (i.e. Baltic Sea) [38]. Regardless of the source salinity of the water, continued distillation without refreshing the feed basin will raise the total TDS. Test show that distillation rates decrease by about 10% as salinity of the source water increases to 200,000 PPM. At these concentrations the water would be salty enough that the user would either empty the brine and start again with relatively lower salt-

concentrate solution, or allow the unit to run dry to remove the salt crystals. Conventional regulated basin systems have the ability to flush brine and add lower salt concentrate when necessary. Such systems usually require some form of electronic or human-guided control, which is beyond the scope of the simplest personal solar stills. The salt concentration of the feed water can rise until the user is forced to some kind of action due to diminishing output. With large-scale systems, control of salt scale is a large concern because the scale can damage transport pipes and systems. In the personal-scale size however, collected salt crystals can be useful for food preservation and can be readily removed by the users since the feed transport mechanisms are simple.

Other concerns are algae and microorganisms, some of which may even be salt-tolerant. This is a significant concern and area of research for reverse osmosis water treatment since these contaminants in the feed water can contaminate the osmotic screens. Pretreatment of water is an important area of research with conventional desalination [38]. Further, conventional biocides can foul the screens as well. These are not a significant problem for solar stills since small amounts of common biocides (such as chlorine bleach, hydrogen peroxide or iodine) can be safely added to feed water, without significant contamination of distillate. Also, hot climates can raise the interior temperatures of solar stills above 65° C, which is usually hot enough to disable the reproduction of bio-contaminants in salt water. On the other hand, cold-weather operation of a solar still can create in internal temperature of the still from 30° – 35° C, which is an ideal temperature range for the production of microorganisms. In this case, salt or common biocides can be added to wintertime feed waters.

9.7 Background on radiance

Thameur, Chaibi, and Bourouni found that the typical global radiation for typical southern Mediterranean conditions varied between 630 W/m^2 during July and 370 W/m^2 during December [30].

Solar radiation is essentially divided into two components: direct radiation from the sun and diffuse radiation, which has been scattered by clouds and dust and arrives from all directions. The relative proportion of direct to diffuse radiation depends on the season and time of day. The diffuse component of total radiation (diffuse + direct) will go to as low as 10% for a clear day and rise to 100% of a much smaller total radiation total for a cloudy day [26]. These authors note that to extract the maximum possible solar radiation, the collector should be arranged at a right angle to the sun's direct radiation.

The solar radiance for a desert climate can go much higher than for a moist or tropical climate due to atmospheric clarity. This is key, because dryer locations can typically benefit from solar desalination. The mean value of solar radiation can reach 1,200 W/m^2 for locations in Jordan [42] with total daily solar intensities reaching 5.6 kWh/m^2/d for northern regions of the country and 6.5 kWh/m^2/d for southern regions.

Typically, daily and hourly radiation intensities are accurately measured using pyrheliometry, but other schemes for estimating radiation intensity have been proposed [38]. For our experiments, we used a solid-state solar radiation measurement system where solar intensity created a current in a photodiode, that was measured and compared to calibrated standards. This produced solar radiance measurements in W/m^2, where the solar intensity was measured constantly, and a mean value was recorded once per minute. This data was then stored in an onboard digital memory, and then

downloaded every several days to a desktop computer. The system was reset and placed in the same location for further measurement. The angle and placement of the sensor replicated as closely as possible the angle and placement of the solar distillation unit.

Howe [38] notes that this wide variation in solar radiation intensity both diurnally and annually requires any useable solar distillation device to be capable of operating at these widely varying intensities and temperatures. The author further notes that the daily production rate of solar distillation equipment will vary by a factor of at least 4 from the winter minimum to the summer maximum. However, we note that when solar desalination units also act as rain-capture devices, some of this variation can be smoothed out through the year, and the addition of water storage to make up for the low-production times and hold rain from the wet months is something that a user of a conventionally-fueled device would not need to consider.

9.8 Output of solar stills

The TDS of the output from a solar still typically is very low, from about 1 PPM – 10 PPM. This is considerably lower than water produced through osmotic methods. The World Health Organization recommends that potable water have a TDS no higher than 500 PPM, so adding ocean water to bring the water up to a more palatable 100 PPM – 200 PPM, could increase the output from a solar still. Research in the United Nations publication examines this process and computes relative costs per liter of distilled water versus costs of this 'cut' water [11].

Typical output rates for basin solar stills are calculated per unit area of basin, which is essentially the footprint of the device. The most common typical output rates was found to be from 2 – 4 L/m^2 per day [35], from a minimum of 1.4 L/m^2 per day [14], and 2 L/m^2 per day [17], and 3.3 – 4 L/m^2 per day [21], up to about 4.15 L/m^2 per day according to Kumar and Bai [14], up to an estimated 5 – 6 L/m^2 per day [13], and 7 L/m^2 per day [27]. Of course, the output of the device is dependent on its location, and high latitudes may be unworkable for solar stills. As a rule of thumb, the workable areas for solar desalination are between the latitudes of 35°N and 35°S, which encompass most of the world's arid zones [23]. Some locations have a relatively low population density, and are in good locations for personal-scale desalination. Tiwari mentions several such countries, which are located close to the equator, including Papua New Guinea, Fiji, Vanuatu, Samoa, Solomon Island, Tonga and New Caledonia [44]. Similar locations exist in the Caribbean, Central America, Africa and Asia. The general cut-off for solar desalination is about 25,000 – 50,000 liters per day [11]. Above this, conventional desalination methods such as reverse osmosis or multi-effect distillation are typically more economical due to land-requirements. Recent advances in osmotic screens have made capacities much lower than these good choices for reverse osmosis, assuming the engineering expertise, parts and energy sources are available. Similarly, advances in UV-resistant polymers and plastic fabrication have made personal-scale desalination systems affordable and workable where they may not have been ten or more years ago. Further, the cost of water distribution needs to be considered for large-scale desalination systems, and where distribution infrastructure does not exist, personal-scale systems may have cost advantages.

Of use in determining the feasibility of a system is the recommended amount of distilled water that a person would need for a day. The World Health Organization estimates that adults need a minimum of two liters of drinking water per day [45]. Larger estimates have been made by Chenoweth, up to 50 liters per person per day, which includes water for drinking, sanitation, bathing and food preparation up to 7.5 liters per person per day as the basic minimum water requirement.

CHAPTER 10

PSPSD EXPERIMENTAL PROCESS

Acrylic panels were manufactured through a thermoforming process as described in this work, using aluminum molds (Figure 10.1) and a heating press. Several of these panels were placed on the roof of the AIME research building, on the campus of the University of Alabama, in a location that is largely free from shadows (Figure 10.2*)*. The panels were exposed to full sunlight and rain. When necessary, the panels were refilled with either fresh water or saltwater depending on the test. Distillate was collected and weighed, as well as analyzed for total dissolved solids.

Figure 10.1 Plastic thermoforming molds

Figure 10.2 Rooftop test array

10.1 Data collection

We took measurements from the panels with fairly simple digital tools. To record the changing solar radiant flux in watts per square meter we used the solar data logger SDL-1 from Micro Circuit Labs. For most of the experiment we set the logger to record an average reading every 60 seconds. This led to a considerable amount of data, so to make analyses easier we later adjusted the meter to record an average reading every five minutes. The data logger was placed on the roof next to the panels, and data was downloaded from the logger to a computer approximately 2 – 4 times per month. The logger is essentially a small, calibrated photovoltaic, which produces a current when exposed to sunlight. The current the cell produces is measured across a known resistance. The current varies with solar intensity, and this value is then correlated to solar radiant flux in watts per square meter, by the instrument's manufacturer, then compared to a known calibrated standard. The current is measured rather than the voltage because this value is less sensitive to heating on the surface of the photo cell.

Distillate was measured by weight with a digital scale, temperatures were recorded with a digital infrared thermometer and a electrical conductivity TDS meter by HM Digital, model COM-100.

10.2 Test unit configurations

The rigid acrylic panels were configured in the following ways:

1. Control – This is the basic thermoformed acrylic panel. The total area of the panel basin area is 84 cm × 70 cm, but the actual evaporation basin area is composed of three channels, each of an area 50 cm × 19 cm, for a total evaporation area of 2850 cm^2. The extra area of the panel is used for optional rain collection, and internal collection channels, which collect the condensate which drips down from the clear barrier (Figure 10.2.1). The evaporation channels are approximately 4 cm deep in standard configuration. The bottom basin is composed of food-grade acrylic plastic, 40 mil thick (approximately 1 mm). The top component of the system is composed of 40-mil clear food-grade UV-hardened acrylic plastic, formed to snap onto the bottom evaporation tray. The top is composed of an 'E'-shaped tower, approximately 12 cm high, with each channel covered by a double-slope leading to the collection channels. The front of the top component folds over the front of the evaporation tray to allow raw water to enter the unit without contaminating the collection channels. At the apex of each tower is a narrow channel to distribute feed water, which can be configured to cool the evaporation barrier (Figure 10.2.1).

2. Anti-condensate coating – This is identical to the control panel, but with an application of anti-condensate spray applied to the inner surface of the top clear barrier. The anti-condensate coating is manufactured by Mardenkro as a concentrated liquid, which was cut with water approximately 40 to 1 for spray application. This anti-condensate contains a natural FDA-approved material (similar to a soluble wax), which reduces surface tension on the plastic, and thus prevents the formation of droplets of condensate. Rather than collect as droplets on the condensation surface, the water sheets to a thin layer and drips into the collection channels. The perceived advantage of this is that the surface is kept clear of droplets, which may reflect a portion of the incoming sunlight and lower the efficiency of the device. We sprayed the solution onto the plastic with a handheld sprayer and allowed the application to sun dry, as directed by the manufacturer.
3. Rock basin – The evaporation basin was filled with dark red and brown lava rocks. These both act as additional thermal mass to hold heat, and they increase the effective surface area of the raw water, which presumably increases the evaporation rate. The rocks are partially submerged in the water and the capillarity of the water in the fine surface channels of the rocks allows the water to creep up the side of the rocks and mostly wet the entire surface of all the rocks (Figure 10.2.2).
4. Rigid foam insulation – This is rigid foam insulation approximately 2 cm thick and is applied to the outside bottom of the evaporation tray. The insulation is

rated R-4. It also serves to increase the rigidity of the panel bottom and prevents deformation of the basin due to the weight of the raw water and stones.

5. Surfactant basin – A small amount of common household surfactant (liquid soap) was added to the raw water in an attempt to lower the surface tension of the water in the evaporation tray, which would presumably allow for an increased evaporation rate.
6. Barrier cooling – The top panel was designed to be cooled with incoming feed water, by flowing over the top (outside) of the condensation surface and then down the sides of the condensation surface into the evaporation tray. The excess water spills over a front barrier and is then recirculated by a solar-driven pump over the surface of the unit. The goal of this method is to the lower the temperature of the condensing surface, which would increase the thermodynamic efficiency of the unit. Unfortunately, the continuous flow of water adds to the basin water and some mixes with the heated water, which also leads to reduction of the temperature of the feed water, and may offset any advantage of cooling the condensation surface. Additionally, the setup requires the use of a shallow basin, which alone adds to the efficiency of the system since less water is required to be solar heated inside the unit, but the overall complexity of the system is increased due to the solar-operated pump and recirculation system.
7. Rigid foam insulation with rock basin, full basin – This combines the rigid foam insulation and rocks in basin.
8. Rigid foam insulation with rock basin and anti-condensate coating – This combines these three.

9. Rigid foam insulation with rock basin, shallow basin – In this case the basin is configured as shallow, with rocks and rigid foam insulation. The advantage of a shallow basin is that the efficiency is presumably increased due to the lower volume of raw water in the evaporation tray. However this necessitates either more frequent filling of the system with raw water or an automated solar pumping system.
10. Fiberglass insulation with rock basin, and shallow basin – In this case the rocks and shallow basin was combined with thick fiberglass insulation instead of rigid foam. The fiberglass insulation offers increased insulation efficiency of R-13 compared to R-4 of the rigid foam. But there is no convenient way of sealing the insulation off from rain leaks, so some of the efficiency is lost as rain collects in the insulation fibers.
11. Fiberglass insulation with rock basin, and full basin – Same as previous but with full basin.
12. Fiberglass insulation with felt basin - In this case, the fiberglass insulation is paired with rolls of dark green synthetic felt placed in the evaporation tray. The purpose of the felt is to increase the effective surface area of the water in the evaporation tray since the felt has a fibrous surface with the water able to spread into the capillarity of the fibers. Unlike the rocks, the felt does not add significant thermal mass.
13. Control with shallow basin – Same as control, but with front basin drain open which creates a basin depth of about 2 cm and correspondingly lower total volume of water in evaporation basin.

14. Rigid foam and adhesive insulation with foam/felt basin – This improves the R-4 insulation of the rigid foam by adding an R-1 layer of flexible adhesive foam between the rigid foam and the outside bottom of the evaporation tray. The synthetic felt is improved with this setup because rather than rolls of the felt, we constructed pads where each felt pocket was filled with about 2.5 mm of open cell foam. This foam acted as a sponge and held the felt directly above the water-saturated layer, that created an improved wicking surface over the felt rolls, which were partly submerged in the water at the edges of each roll.
15. Rigid foam and adhesive insulation with foam/felt basin and saltwater – This is identical to the setup with rigid foam and adhesive insulation with foam/felt pads, except that this unit was filled with saltwater of approximately 30,000 PPM rather than freshwater.
16. Control basin with saltwater, unit 1 – This was identical to the control setup, except that it was filled with approximately 30,000 PPM saltwater instead of freshwater.
17. Control basin with saltwater, unit 2 – This is identical to Control basin with saltwater, unit 1, for additional control and error analysis.

In addition to the rigid acrylic basins, there were also variations on the polyethylene basins:

1. Control, standard polyethylene basin – This is a single basin solar still, which is constructed of 6-mil (0.15 millimeter) thick polyethylene plastic. The unit is made of a bottom portion composed of black polyethylene, reinforced with

polyethylene threads in a diamond-grid pattern, and a top portion which is UV-hardened clear polyethylene with an anti-condensate coating on the inner surface and an infra-red reflecting coating on the outside surface designed to allow additional IR energy to the inside of the unit and increase the thermal efficiency. The front of the clear panel has a fold, which collects the condensation, which drips down the inside of the unit toward the front. The condensate is collected in this fold and channeled to a fitting, which then runs the collected distillate to an external carboy. The anti-condensate coating is deposited by the plastic manufacturer and is designed to eliminate droplets on the inner surface and sheet the water to the collection channel. The flexible unit is held in shape by narrow-gauge PVC tubing typically used for household water supply. The unit is filled with raw water through a zipper in the back of the unit, (Figure 10.2.3).

2. Small polyethylene basin - This is identical to the control, but smaller in size.
3. Foam/Felt basin with insulation - This is identical in size and shape to the control, but the evaporation basin is fit with an evaporation pad made of a pouch of synthetic felt filled with a layer of approximately 2.5 cm open cell foam. The pad is designed to stabilize the water and increase the evaporation of the feed water by increasing the surface area and lower the effective surface tension due to the fabric's capillarity.

Figure 10.2.1 Rigid acrylic panel

Figure 10.2.2 Rigid acrylic panel with rock filled basin

Figure 10.2.3 Flexible polyethylene panel

CHAPTER 11

PSPSD MODIFICATIONS TO BASIC DESIGN

In this section we examine modifications that we made to our proprietary acrylic and polyethylene personal-scale solar stills. All trials were referenced to a control and were conducted on the aforementioned roof of a building on the campus of the University of Alabama. After these we examine the flexible polyethylene still and variations and reference them to the acrylic panel control.

In order to test the effects of various modifications and configurations of several single basin solar stills, we conducted field trials on identical sets of stills, with various modifications on different stills. The still tests were largely broken into two sets of tests: acrylic panels and poly panels. The acrylic panels are pressure-formed acrylic panels made of UV-hardened, food-grade acrylic. The poly panels are made of heat-seamed UV-hardened, food-grade roll polyethylene. Both panels are composed of black bottoms and clear tops, and both essentially have single basins, however the acrylic panel's basin is divided into three compartments to facilitate brine collection.

The following subsections compare first the rigid acrylic panels (RAP) and then the flexible polyethylene panels (FPP).

11.1 RAP, anti-condensate

We conducted a test with a standard acrylic panel, and applied an anti-condensate coating to the inner surface. The coating is made by Mardenkro, under the name Anti-Condens and the concentrated solution was diluted with 40 parts water per 1 part anti-

condensate concentrate. The spray was allowed to dry, and the top of the panel was replaced. The purpose of the spray is to prevent large droplets from forming on the inner surface of the condensation barrier. It was hoped that this would allow greater sunlight penetration into the unit and increase the efficiency of the solar process. The coating acts as a surfactant to sheet the condensed water off the surface and into the collection channel.

After application it was noticed that large droplets did not form on the inner surface of the panel as they did in the untreated units. However the average thermodynamic efficiency recorded over 18 days showed no significant difference between the unit with anti-condensate coating and the control. In fact, the untreated control produced an average of 37% more output and 41% more grams per unit W/m^2 than the treated unit.

We did not expect the coating to decrease the output of the device, and these differences seem large enough to attribute to something more than error. We do not completely understand why the anti-condensate coating reduced the output, but the fact that the thermodynamic efficiency was similar for both suggests that possibly the water droplets which collect on the inner surface of the bare condensation barrier may help to insulate the unit by reducing heat loss through the top barrier. It also suggests that coating may inhibit the formation of condensation on the inner surface.

11.2 RAP, rock-filled basin

In a lightweight, personal-scale solar still, inserting stones in the evaporation channels serves three purposes. (We used dark red and dark grey lava rocks, which are extremely porous and lightweight.)

1. The stones increase the effective surface area by allowing the basin water to seep up in to small cracks and pits of the stone surface.
2. The stones hold in heat and by acting as a heat mass, they increase the output of the still and allow the still to continue to produce water after the sun goes down.
3. The stones stabilize the units in high winds.

We followed the example of Abdallah, Abu-Khader and Badran [42]. The obvious benefit of using dark stones as an enhancement to the solar still is that stones are available nearly everywhere in the world. We used dark red and dark grey volcanic lava rocks which unlike smooth stones offered a lot of sponge-like porosity to increase surface area of the evaporation basin.

The stones increased the thermal efficiency by 1% to 2% over control through trials conducted from 9/30/09 to 10/6/09. The still with the stones increased the output per unit radiance by 33% over control and it increased the output in liters per day by 47% over control. We were encouraged by these significant results since the relatively modest increase in thermal efficiency seems to be only partly responsible for the increased output, and at least part of the increased output seems to be a function of the wetting surface of the stones.

11.3 RAP, insulated basin (thin)

The next experiment was to measure the effect of insulating the bottom of the solar basin with a thermal insulator to hold in heat and presumably increase output after the sun goes down. For this experiment we used ¾-inch rigid foam board insulation with an insulating value of R-4. This proved to be a workable choice for insulation because rainwater drained off and was not absorbed by the insulation.

The thermodynamic efficiency of this setup improved by 1% over the control. The water output per unit radiance improved by 48% over control and the water per day increased by 41% over control. We later combined this type of insulation with other improvements outlined here. While not as cheap a modification as the stones, this modification offers a lot of return for the investment because the cost per unit area for the insulating foam is considerably lower than the cost per unit area of the still material. A good future test for insulating materials might be materials that can be found easily in Developing Nations, such as dry grass and bark.

11.4 RAP, basin with surfactant

A small amount of common surfactant (household soap liquid) was added to the evaporation basin to test the ability of a surfactant to lower surface tension of the evaporation basin, which we hoped would improve efficiency by allowing evaporation to occur with slightly less energy input since surfactants lower the surface tension of the feed water.

Average thermodynamic efficiency did not significantly change for the surfactant trial over control. There was a measured increase in average output, with the surfactant

trial producing about 6% more distillate than control, but this increase came with the cost of some of the soap ending up in the distillate. Given the modest increase in distillate output and the side effect, we do not plan to investigate surfactants further.

11.5 RAP, barrier cooling

In this test we used a design feature of our plastic solar still, where water is fed into the unit by running the cooler feed water over the outside of the clear condensation barrier. In theory, this cool water can reduce the temperature of the condensation barrier, which will increase the thermodynamic efficiency. With our design, the water cool water also mixes slightly with the heated basin water before being recirculated, this lowers the temperature of the feed water slightly, which lowers the thermodynamic efficiency. Our tests indicate a negligible difference in thermodynamic efficiency between the barrier-cooled setup and the control. However, the barrier-cooled setup produced about 44% more water than the control. We suspected this may be partly due to the smaller basin of the barrier-cooled configuration because the front drain was opened to allow recirculation of the water, while on the control it was closed which led to an effectively larger basin. To test this, we created a configuration with the same effective basin size as the barrier-cooled configuration, but without the barrier cooling.

11.6 RAP, insulated basin (rigid foam) with rocks (trial 1)

We combined the rigid foam insulation with rocks. This improved the thermodynamic efficiency by an average of 1% over the control, and increased the liter per day output by an average 110% over the control.

11.7 RAP, insulated basin (rigid foam) with rocks, AC

We combined the rigid foam insulation with rocks and anti-condensate coating on the condensation surface. The thermodynamic efficiency was increased to an average of 1% over the control, and the output in liters per day increased by 110% over control. However, the anti-condensate coating did not seem to offer an improvement in output over the same setup without the coating. This corresponds to the result we had when we used anti-condensate without the insulation and rocks, and we will compare these two setups separately.

11.8 RAP, insulated basin (rigid foam) with rocks (trial 2)

As part of a new set of trials, we reproduced this setup since it offered the most promising results from our first set of trials. We found results similar to the same setup with trial 1. The insulated with rocks setup increased thermodynamic efficiency by an average of 2% over control, and increased liter per day output by an average of 93% over control. This is lower than our first trial, but they were tested with lower total radiance.

11.9 RAP, insulated basin (fiberglass) with rocks (full basin)

For this setup we insulated our panels with fiberglass, which initially provided an R-value about 3 times higher than the rigid foam. However, this decreased after time because rainwater got into the fiberglass. Because of our inability to protect the fiberglass insulation from rain we concluded that this type of insulation is unworkable even though there initially seemed to be a thermal advantage with the higher R-value.

The fiberglass insulation with rocks gave an average of 1% improvement of thermal efficiency over the control, and an increase of an average 112% liters per day over the control.

11.10 RAP, insulated basin (fiberglass) with rocks (shallow basin)

This setup was similar to the Insulated basin (fiberglass) with rocks; however this setup used a basin with the front drain open, thus the basin water volume was reduced by approximately half. The decreased water in the basin should typically add to the efficiency of the process, since there is less water to solar heat. However, less water also means less thermal mass to continue to produce water after the sun goes down, thus there is some added complexity, and we will compare the full basin to shallow basin later.

This setup produced an average thermal efficiency 2% higher than the control, and produced average liters per day 113% higher than the control.

11.11 RAP, shallow basin

In order to get an idea of the difference of using the shallower basin configuration, and quantifying some of the results of the shallow basin configuration with other setups, we conducted a test of a shallow basin control. This setup was identical to the control except that it used a shallow basin.

It had an average thermodynamic efficiency of less than 1% difference from the control, but it produced an average of 30% more water in liters per day than the control. While the extra output was advantageous, the extra difficulty with maintaining the shallow basin may negate this advantage. Specifically, the thin basin configuration

requires that the feed tray be filled more often since it holds about half of the volume of water as with the full basin setup. The salt concentration in the brine increases more quickly as well, which will necessitate more frequent removal of salt crystals.

4.12 RAP, insulated basin (fiberglass) with felt evaporation surface

Using rocks as a thermal mass and as a means to increase effective surface area is advantageous in that it uses locally-available material, but as the salt concentration increases in the brine pool it becomes difficult to run the unit dry in order to remove the crystallized salt. Following the work of Abdallah et al. [42], we placed rolls of wicking felt in the basin so that the top parts of the horizontally arranged tubes were raised out of the basin. The wicking surface draws water up the fine threads in the fabric and decreases the effective radius of curvature, which increases evaporation.

The advantage of using wicking foam over rocks is that the units can be configured quickly without the need to source locally-available dark stones, and the pads can be quickly squeezed to remove brine and the unit can run dry when salt concentration in the brine is high, in order to remove crystallized salt.

The basin was insulated with fiberglass insulation. Compared to the control, this setup produced a thermodynamic efficiency that averaged 2% higher. These setups produced an average of 69% more liters per day than the control during the same period.

4.13 RAP, insulated basin (rigid foam) with felt wicking pads

Because of the reasonable success of the rolls of wicking material, we examined this process further, and constructed wicking pads, where a shell of the wicking felt was

sewn around a open cell foam. The foam held the water while allowing the wicking material to draw water up from the foam. The foam also kept an ideal shape for the wicking material, allowing it to remain the correct height above the water basin, which essentially replaced the open water basin with a water-filled foam basin.

The insulation on this trial had a higher R-value than previous trials that used rigid foam. In this case, R-1 adhesive thermal foam with reflective IR barrier was placed between the bottom of the still and the rigid insulation, which was R-4.

This setup produced a slightly lower thermal efficiency than the control, by an average of 0.4%, but it produced an average of 123% more water than control in liters per day. This setup performed similarly to the test with rigid foam insulation and rocks.

11.14 RAP, saltwater control

Due to the difficulty of maintaining consistent salinity as the feed water evaporated, we chose to run our tests with freshwater. However we tested three different experimental setups and compared them to the theoretical predication of decreased output with highly saline water. The total dissolved solids (TDS) in parts per million (PPM) for the freshwater was between 70 and 120 PPM. The TDS and PPM for the saltwater was approximately 35,000, a salinity typical to ocean water.

We set up two solar evaporation panels as direct salt-water counterparts to our control, with the same operating parameters and configuration, except that both were filled with saltwater instead of freshwater. The thermodynamic efficiency of both panels differed from the control by an average increase of 1%. As predicted by theory, the output was less for the salt-water panel by an average of 6% less in liters per day.

The typical operation of these panels in the field is to continually add raw water to the panel as necessary. In doing so the salinity of the feed water continually increases which steadily decreases output of fresh water. In typical operation, the water would reach approximately 100,000 PPM (10% salt) in approximately a month, at which point the brine would either be removed or allowed to dry and the salt to crystallize. The unit would then be refilled with seawater.

We also tested a saltwater variation of the panel with rigid foam insulation and foam wicking pads. The saltwater version of the panel produced an average of 87% more water than the control compared with an increase of an average of 123% more than the control from the same panel (rigid foam and foam wicking pads) but filled with freshwater. So the salt seemed to significantly affect the efficiency of the insulated wicking panel, however we need more data on this, because the more than 30% average difference in output between the freshwater wicking system and the saltwater wicking system seems excessive, given the much smaller difference from the controls. This system also has insulation; it sits on an R-4, rigid foam, 2.5 mm thickness pad.

11.15 FPP, small poly unit vs. poly control

Thermodynamic efficiency was similar to the control unit at 4%. Since both units primarily differ only in size, this makes sense. When the output is corrected for area, the control produces 15% higher output. This may be a function of the higher thermal mass in the larger unit.

11.16 FPP, foam/felt poly unit vs. poly control

The foam/felt unit differed from the control only in the add-ons. The foam/felt unit has a basin-sized wicking pad and rigid foam ground insulation. The size and still construction are identical however, which allows us to do direct comparison. The foam/felt unit has a similar thermodynamic efficiency to the control, but produced 153% more distillate in the same time period as the control. The foam/felt unit also had a 106% increase in output per unit area over the control. It seems that the wicking surface produces a very obvious and worthwhile improvement to the solar still approaching the increased efficiency of a tilted wick still. However modification is simple, the wicking pad is just inserted into the unit, rather than requiring an extensive redesign typical to tilted-wick stills.

11.17 FPP, control poly unit vs. control acrylic unit

In this case both units are obviously different sizes, but the poly control has a 112% increase in distillate per unit still area over the rigid acrylic control. Average thermodynamic efficiency was 2% higher than the poly control unit over the rigid acrylic control.

11.18 FPP, foam/felt poly unit vs. control acrylic unit

The flexible unit with wicking pad installed produced over 235% more distillate per unit area than the control unit for the rigid PVC panels. This comparison is useful because it demonstrates the value of the wicking surface and insulation.

11.19 FPP, foam/felt poly unit vs. foam/felt acrylic unit

In this case, the poly unit with the wicking pad and rigid ground insulation is compared to the similarly equipped rigid acrylic version. The total evaporation area of the poly unit is approximately four times the rigid acrylic's evaporation area, but adjusting the output for area shows that the flexible poly unit still beats the similarly-equipped rigid acrylic unit by 33% output per unit area, and with a similar thermodynamic efficiency.

11.20 FPP, foam/felt poly unit vs. rocks/insulation acrylic unit

Although the foam/felt and rock units are of fundamentally different construction, their comparison is useful because the rock-filled rigid panels may offer the most economical and practical way of deploying the rigid units in Developing Nations. The rigid unit filled with stones offers a clear thermodynamic advantage, since the flexible panel with the wicking pad produced similar thermodynamic efficiency. Still, the flexible units beat the rigid acrylic units for output by an average of 75% when adjusted for area, compared to about 33% for the rigid panels with wicking pad.

11.21 FPP and RAP summary

Conclusions of the different systems will follow in the next sections, but in summary, we found that the foam/felt evaporation surfaces improved desalination efficiency most for both FPP and RAP systems. Even when the foam/felt surface didn't have a thermodynamic advantage over other methods, it still produced more distillate, likely due to the superior evaporation surface.

CHAPTER 12

PSPSD DATA

Table 12.1 Relevant data for calculation of performance ratio

Date/Time	Tot. Radiance W/m^2	Tot. Daylight Min	Tot. Night Sec	Avg. Radiance	Tot Daylight Sec.	Avg Rad W/m^2•s	Total Solar Energy, RD, J	Total Solar Energy, SEAP, J	After dark minutes	Avg. Temp °C	Hi Temp °C
9/2/2009										24	28
9/3/2009	316235	753	59700	420	45180		2.2E+07	5E+06	1048	23	28
9/4/2009	350689	735	25200	477	44100	7.95	2.5E+07	6E+06	752	24	32
9/8/2009	760377	2432	172260	313	145920	5.21	5.4E+07	1E+07	2429	24	24
9/13/2009	1115547	3382	219660	330	202920	5.50	7.9E+07	2E+07	3376	25	30
9/13/2009	101453	581	5820	175	34860	2.91	7182844	2E+06	677	25	29
9/15/2009	367634	1305	81420	282	78300	4.70	2.6E+07	6E+06	1304	25	30
9/16/2009	255139	783	58800	326	46980	5.43	1.8E+07	4E+06	1015	26	32
9/17/2009	198308	693	31680	286	41580	4.77	1.4E+07	3E+06	693	25	29
9/18/2009	272	14	24180	19	840	0.32	19222.2	4496	356	25	29
9/22/2009	684547	3022	213120	227	181320	3.78	4.8E+07	1E+07	3022	24	28
9/23/2009	294118	856	46380	344	51360	5.73	2.1E+07	5E+06	856	26	31
9/24/2009	142613	414	44700	344	24840	5.74	1E+07	2E+06	414	27	31
9/24/2009	120675	304	780	397	18240	6.62	8543797	2E+06	318	27	31
9/25/2009	457	27	43800	17	1620	0.28	32348.5	7566.3	27	27	31
9/25/2009	275548	675	1380	408	40500	6.80	2E+07	5E+06	697	27	33
9/27/2009	240804	963	89040	250	57780	4.17	1.7E+07	4E+06	963	24	29
9/29/2009	525687	1101	67740	477	66060	7.96	3.7E+07	9E+06	1101	24	29
9/30/2009	724327	1171	68220	619	70260	10.31	5.1E+07	1E+07	1171	17	24
10/1/2009	384561	847	48060	454	50820	7.57	2.7E+07	6E+06	874	19	26
10/2/2009	291404	590	44520	494	35400	8.23	2.1E+07	5E+06	590	21	27
10/3/2009	374250	772	50220	485	46320	8.08	2.6E+07	6E+06	855	18	26
10/6/2009	142691	1485	140400	96	89100	1.60	1E+07	2E+06	1485	17	20
10/8/2009	381701	1362	93960	280	81720	4.67	2.7E+07	6E+06	1362	23	28
10/9/2009	384184	1013	47940	379	60780	6.32	2.7E+07	6E+06	1040	25	32
10/13/2009	228533	2062	189300	111	123720	1.85	1.6E+07	4E+06	2062	18	20
10/14/2009	111105	742	55560	150	44520	2.50	7866241	2E+06	742	21	26
10/14/2009										21	26
10/16/2009	145476	1423	91380	102	85380	1.70	1E+07	2E+06	1423	17	21
10/19/2009	790345	2042	143700	387	122520	6.45	5.6E+07	1E+07	2042	10	15
10/21/2009	332166	702	95100	473	42120	7.89	2.4E+07	6E+06	702	13	22
10/22/2009	276876	730	47400	379	43800	6.32	2E+07	5E+06	730	16	24
10/22/2009	214038	487	4260	440	29220	7.33	1.5E+07	4E+06	557	21	26
10/23/2009	4087	86	46560	48	5160	0.79	289367	67682	86	21	26
10/25/2009	838708	1800	98640	466	108000	7.77	5.9E+07	1E+07	1825	12	19
10/26/2009	223221	635	48660	352	38100	5.86	1.6E+07	4E+06	635	14	21
10/28/2009	373781	1193	99600	313	71580	5.22	2.6E+07	6E+06	1202	17	19
10/29/2009	188593	599	50400	315	35940	5.25	1.3E+07	3E+06	611	21	28
10/30/2009	108999	487	48060	224	29220	3.73	7717094	2E+06	487	23	28
10/31/2009	195368	751	68340	260	45060	4.34	1.4E+07	3E+06	1059	13	17
11/2/2009	654643	1233	75960	531	73980	8.85	4.6E+07	1E+07	1233	12	20
11/4/2009	315936	728	98820	434	43680	7.23	2.2E+07	5E+06	728	15	23
11/4/2009	315499	513	1260	615	30780	10.25	2.2E+07	5E+06	533	15	23
11/5/2009	103631	257	48300	403	15420	6.72	7337082	2E+06	257	14	22
11/6/2009	539713	968	49740	558	58080	9.29	3.8E+07	9E+06	968	13	22
11/8/2009	555049	1221	100020	455	73260	7.58	3.9E+07	9E+06	1240	15	24
11/9/2009	72958	578	53220	126	34680	2.10	5165441	1E+06	649	18	22
11/11/2009	293631	1135	101700	259	68100	4.31	2.1E+07	5E+06	1135	16	18
11/12/2009	302087	613	57720	493	36780	8.21	2.1E+07	5E+06	679	13	20
11/13/2009	293045	594	43260	493	35640	8.22	2.1E+07	5E+06	597	12	22
11/15/2009	218594	1070	100320	204	64200	3.40	1.5E+07	4E+06	1070	13	21
11/17/2009	193664	1215	101880	159	72900	2.66	1.4E+07	3E+06	1215	13	19
11/20/2009	240941	1793	152070	134	107550	2.24	1.7E+07	4E+06	1793	12	19
11/25/2009	141361	2813	265230	50	168750	0.84	1E+07	2E+06	2813	12	18
12/9/2009	419024	7915	739800	53	474900	0.88	3E+07	7E+06	7941	11	16
12/11/2009	81211	1105	102360	73	66300	1.22	5749760	1E+06	1105	9	16
12/14/2009	17121	1610	166320	11	96600	0.18	1212131	283515	1677	9	15
12/20/2009	128532	3205	318180	40	192300	0.67	9100073	2E+06	3205	9	14
12/21/2009	65326	655	53040	100	39300	1.66	4625102	1E+06	655	8	14
12/22/2009	52373	575	51900	91	34500	1.52	3708023	867300	575	8	14
12/29/2009	265772	3995	365400	67	239700	1.11	1.9E+07	4E+06	3995	8	13
1/15/2010	808669	1946	1352820	416	116760	6.93	5.7E+07	1E+07	1946	0	6
1/18/2010	61684	1675	160740	37	100500	0.61	4367241	1E+06	1675	10	15
1/21/2010	88558	1775	155580	50	106500	0.83	6269899	1E+06	1775	13	20
1/22/2010	16795	600	47460	28	36000	0.47	1189051	278117	600	13	19
total/averages			**7529040**		**4728300**		**2.1E+07**	**5E+06**			

These correspond to readings taken at each test unit throughout the trials over the indicated time period. The complete data are available in digital form for further examination and analyses.

CHAPTER 13

PSPSD ANALYSIS

We needed to analyze the relative efficiencies of the different systems in a way that was compatible with our data-taking. One of the limitations of experiments like these is the expense and difficulty in obtaining real-time in-situ temperature data from several sources. If cost were not a barrier, we would have installed thermal data loggers into each unit, and measured distillate as it was produced. While this may have been feasible for one or two test units, it wasn't feasible for us to do this with several test units. As such, we measured temperature and output at sporadic times, and we attempted to take representative data.

13.1 Novel analysis: Performance ratio

This temperature data could be used to compute maximum thermodynamic efficiency, through the Carnot relationship, where T_c is the temperature of the cooler condensation surface in K and T_b is the temperature of the hotter basin in K

$$e_{\text{therm}} = 1 - \left(\frac{T_{\text{c}}}{T_{\text{b}}}\right). \qquad \text{(Eq. 13.1.1)}$$

When we applied this to our actual measured results we found that our units with comparable thermodynamic efficiency often produced very different amounts of distillate per unit area in the same conditions. One of the goals with our solar desalination research is to compare different sized stills, of different construction and features under different conditions to attempt to find still innovations that offer increased performance. However the use of thermodynamic efficiency as a measure of a still's efficiency is not pertinent

for us as demonstrated by our research. We thus examined an alternate method of evaluating still performance based not on the still's operating temperature but rather on the still's exposed solar radiance. Solar radiance is one of the least expensive, simplest quantities to measure in-situ. One small data-logging solar incident meter (SIM) can record radiance (in W/m^2) for several test units. Due to the simplicity of this circuit, weather-proof, data-logging SIMs which are calibrated to the U.S. Bureau of Standards, and can be purchased for less than $200, making them ideal as a field measurement device. We therefore computed an alternate performance ratio based on the solar energy received at the surface of the panel (i.e. measured by the SIM) and related it to the distillate that it produced. We believe that this method is more workable and more useful than thermodynamic efficiency for measuring solar still efficacy. Further, it allows data to be collected from disparate locations and compared and analyzed.

The values measured *in-situ* are:

1. R – Solar Incident Meter measures solar radiant flux in units of W/m^2, digitally sampled. (We chose to sample in 1-minute increments, and later 5-minute increments.)
2. T_c – Temperature of condensation barrier (i.e. cold), measured with a handheld infrared thermometer, in degrees C, converted to K for calculations.
3. T_b – Temperature of evaporation tray (i.e. hot), measured with a handheld infrared thermometer, in degrees C, converted to K for calculations.

4. t – Time of day and date, recorded by SIM and also hand-recorded on measurements 2, 3, 5, and 6 above, converted to seconds.

5. m_d – Measurement of distillate output (in grams) by portable digital balance.

6. Total dissolved solids in distillate and feed water (in PPM) by portable TDS meter.

7. T_{day} – Average daily temperature, in degrees C, recorded at the nearest weather measuring station. We obtained ours from the National Weather Service, from an affiliated measuring site located a few miles from our point of measurement.

From this data we can build a complex model describing the operation of a unit, an array of units or units in disparate locations and times. First, we want to find the average fractional increase in temperature $\Delta\overline{T}_{\text{still}}$ inside of the basin due to the greenhouse effect. To find this we define

$$\Delta\overline{T}_{\text{still}} = \frac{\left(T_{\text{b}} - T_{\text{c}}\right)}{T_{\text{b}}}. \qquad \text{(Eq. 13.1.2)}$$

Then, using this we can use $\Delta\overline{T}_{\text{still}}$ to compute the average estimated internal temperature *increase* $\overline{T}_{\text{incr}}$ inside of each unit,

$$\overline{T}_{\text{incr}} = \overline{T}_{\text{day}}\,\Delta\overline{T}_{\text{still}}, \qquad \text{(Eq. 13.1.3)}$$

can be used to find the average basin temperature $\overline{T}_{\text{b}}$,

$$\overline{T}_{\text{b}} = \overline{T}_{\text{incr}} + \overline{T}_{\text{day}}. \qquad \text{(Eq. 13.1.4)}$$

This process is shown in Table 13.1.2. (The average basin temperature can also be measured through the day with an in-still temperature data-logging system, if the

experimenter is capable of taking these measurements. We were not equipped to do so, however.)

Applying conservation of energy and thermodynamic energy, we define m_c as the theoretical mass of distillate in grams predicted by conservation of energy and thus,

$$m_c = \left(\frac{Q_{total}}{C\left(100 - \bar{T}_{\text{basin}}\right) + L} \right) \cdot 1000 , \qquad \text{(Eq. 13.1.5)}$$

where L is the latent heat of vaporization, C is the specific heat, and Q_{total} is found from our measured data. R was recorded at the SIM every minute, and A is the basin area in units of m^2, thus we convert to an average value per second,

$$Q_{total} = \left(\frac{R}{\left(t/60\right)} \right) At = RA(60) . \qquad \text{(Eq. 13.1.6)}$$

Then, a performance ratio Γ can be determined,

$$\Gamma = \frac{m_d}{m_c} . \qquad \text{(Eq. 13.1.7)}$$

For comparison, we computed both the thermodynamic efficiency and the performance ratio over the range of measurements using mean values and compiled them into Table 13.1.2.

Table 13.1.1 Estimated average temperature increase due to greenhouse effect

Determination of avg temp increase in enclosure			
Date/time	**cover temp °C**	**basin temp °C**	**Difference**
10/30/09 15:30	31.7	37.8	19.3%
11/5/09 10:50	26.7	38.9	45.8%
11/8/09 16:55	21.7	28.9	33.3%
11/15/09 14:22	39.4	48.9	23.9%
11/17/09 14:55	22.2	35.6	60.0%
11/20/09 15:02	28.3	39.4	39.2%
11/25/09 15:35	26.1	37.8	44.7%
12/20/09 14:41	22.8	35.6	56.1%
		avg diff	40.3%

Table 13.1.2 Comparison of performance ratio with thermal efficiency

Thermodynamic Efficiency compared to Performance Ratio	**Performance ratio**	**Therm. efficiency**
1 RD3	15%	4%
2 RD3 felt	21%	4%
3 SP_control	18%	2%
4 SP_1_A.C.	14%	2%
5 SP_rock	22%	2%
6 SP_thin insulation	21%	3%
7 SP_surfactant	16%	2%
8 SP_barrier cooling	19%	2%
9 SP_thin insulate_rock	26%	3%
10 SP_thin insulate_rock_AC	29%	3%
11 thin insulate_rock_full basin	27%	4%
12 thick_insulate_rock_shallow basin	29%	4%
13 thick/rock/fu	36%	3%
14 thick/felt/fu	23%	4%
15 control/shal	16%	2%
16 thin/newfelt/full*	35%	4%
17 thin/newfelt/salt**	27%	4%
18 control/salt 1	17%	3%
19 control salt 2	21%	3%
**excluded dissimilar data set because sample was small*		
***excluded trials below 0°C; saltwater does not freeze*		

These 19 trials are for a variety of still sizes, configurations, and designs, yet the performance ratio gives us an immediate indication of the still performance that would be difficult to see by using just the thermodynamic efficiency. For instance, trials 1 and 16 have a similar thermodynamic efficiency of 4%, yet, the trial 16 has a performance ratio of over twice that of trial 1. We believe that the use of this performance ratio is a valuable measure of disparate stills, while requiring only modest data gathering techniques and equipment.

CHAPTER 14
PSPSD FUTURE WORK

Our tests were largely performed during the late summer and fall. We continued monitoring the test units after we finished the initial study, and we hope to update these results with the higher output we recorded during the hotter months. In addition, we optimized the geometry of the flexible still with less airspace and a smaller footprint. Initial results have shown that the new design produces about 75% of the output of the full-sized system, but in a system which in about half the size and weight. We would like to optimize the rigid panels as we have done with the flexible panels, given the results of this study, but the costs of mold making and thermoforming is too high to currently attempt this. Similarly, we would like to produce a third design class, based on another patent-pending blow-molded bottle, also owned by the University of Alabama, but again, this will require a new phase of research funding.

Additional work remains to perform analysis on this data and correlate the production rate to the average wind speeds and season, and also refine the theoretical model for latitude and season. The ideal distillate output model should incorporate average solar radiance for various locations and give a predicted output. We also would like to find better correlation between the thermodynamic model and the performance ratio.

Further work remains to improve our model to predict the output with source water of high salinity. Given the design of the simple solar still, the output will decrease by small amounts as additional seawater is added to the basin, because the salinity will

increase with time and correspondingly decreasing output until the high-salt brine is either emptied or the unit run dry and crystallized salt removed.

Characterization of the material used for these stills may prove useful, and would be a good potential area for research. Specifically, it may be useful to know about the relative radiance transmission through the different material choices, and apply these to a model which optimizes the best material choice given the ability to allow light through, the ability to insulate, cost, wetability and durability.

CHAPTER 15
PSPSD CONCLUSIONS

The work of Abdallah et al. [42] proved to be key in this research, because it led us to examine methods of increasing evaporation through both increasing the thermal mass in the water basin and by increasing the evaporation area in the basin. Just as importantly, Abdallah et al. suggested ways to increase output using commonly available materials which did not require modifications to the basic technology.

After our field testing of the units, we found that we could increase the output of our control unit by an average of 93% over the control by filling our evaporation tray with porous lava rocks. These stabilize the unit in high winds and are easily sourced in many locations, especially in the South Pacific. The drawback of using these stones though is that it becomes more complex to manage increasing salinity levels in the evaporation trays when they are filled with rocks. For this reason, we can only recommend the use of rocks for this type of distillation device when the water used is contaminated freshwater, rather than seawater. However, these rocks may prove useful in a conventional solar still where the basin water is continuously refreshed with relatively low salt or brackish water, less than 5,000 PPM.

We also found that the felt-wrapped foam slabs proved to be the most productive, increasing output over the control by an average of 123% when combined with rigid foam insulation. Unlike the rocks, these do require slightly more specialized manufacturing, but these ‘pillows’ are lightweight and could be easily shipped with the panel. Also unlike the rocks, they are compatible to brine water in the evaporation tray. When the salt levels get too high and output decreases, the ‘pillows’ can be squeezed out

and removed, and the units can be run dry, then the salt then scooped out and repurposed or disposed. The units can also run dry with the 'pillows' in place, after which they can be removed and the salt shaken off. The additional thermal mass of these largely void-filled foam blocks is relatively negligible compared to the thermal mass of the water in the basin. Therefore we conclude that the increased efficiency of the units is a result of the felt's ability to increase the effective evaporation area of the surface of the water, since water is adsorbed onto the felt's thin fibers, which creates a much lower radius of curvature for the water surface. This then effectively lowers the energy necessary to evaporate a molecule of water from the surface, since the molecule interacts with fewer surface molecules and experiences a lower total necessary energy to break free to the gaseous phase.

We found that some modifications were not worth the trouble and effort. Specifically, attempting to increase the output by adding surfactant to the feed water had little effect. While our barrier-cooling setup was interesting, the additional output was not worth the complexity and expense of adding a recirculating solar-driven pump.

We found that our flexible poly stills had excellent output, and that similar to the rigid acrylic panels, output significantly increased when a felt-wrapped foam block was inserted into the evaporation basin and a layer of rigid insulation foam was placed between the bottom of the panel and ground (or rooftop, in our case).

In addition to these improvements, we found that rigid foam is the best choice for insulation because it is manageable, inexpensive and unlike fiberglass insulation it doesn't absorb rain water. We used ¾-inch thick R-4 rigid foam insulation and found that the insulated panels had an increase of about 40% over the control.

Finally, we were encouraged by the method of predicting the theoretical output of our devices using basic measurable assumptions. Correlation with measured results was good and we believe that with additional refinements, this method may prove useful as a predictor of solar still outputs in a way that is dependent on measurement of incident solar radiation rather than temperature measurements in and on the still.

REFERENCES

1. S. Sethi, S. Walker, J. Drewes, P. Xu, Existing and emerging concentrate minimization and disposal practices for membrane systems, *Florida Water Resources Journal*. 38, June (2006).

2. M. Mickley, Membrane concentrate disposal: practice and regulation. *Report No. 69. U.S. Department of Interior, Bureau of Reclamation*, (2001).

3. John J. Wright, Stephen Van Der Beken , The Hall Effect in a Flowing Electrolyte, *Am. J. Phys.*, **40**, 245 (1972).

4. H.S.T. Driver, Comment on The Hall effect in a flowing electrolyte, *Am. J. Phys*. **46,** 1275 (1978).

5. R. De Luca, Lorentz force on sodium and chlorine ions in a salt water solution flow under a transverse magnetic field, *Eur. J. Phys*, **30,** 459 (2009).

6. C.E. Brokaw, et al., Method and apparatus for magnetic separation of ions*, United States Patent*, **7645985**.

7. S.J. Kim, S.H. Ko, K.H. Kang, J. Han, Direct seawater desalination by ion concentration polarization, *Nature Nanotechnology,* advance online publication, 21 March (2010).

8. P. LeClair, *PH255 Modern Physics Laboratory Guide*, self-published, pp. 160 (2010).

9. Engineering Toolbox, http://www.engineeringtoolbox.com/reynolds-number-d_237.html.

10. *Desalination's Future Champions*, Lux Research Inc., Boston, MA, (2009).

11. *Solar Distillation as a means of meeting small-scale water demands*, United Nations Publication, N.Y., (1970).

12. G. Fiorenza, V.K. Sharma, and G. Braccio, Techno-economic evaluation of a solar power water desalination plant*, Solar Desalination for the 21st Century*, Springer, 2217 (2007).

13. B. Bouchekima, A small solar desalination plant for the production of drinking water in remote arid areas of southern Algeria, *Desalination,* **159**, 197 (2003).

14. K.V. Kumar and R. K. Bai, Performance study on solar still with enhanced condensation, *Desalination,* **230,** 51 (2008).

15. A.K. Tiwari, and G.N. Tiwari, Thermal modeling based on solar fraction and experimental study of the annual and seasonal performance of a single slope passive solar still: The effect of water depths, *Desalination,* **207,** 184 (2007).

16. W.S. Gillam and W.H. McCoy, Desalination Research and Water Resources, *Principles of Desalination*, Academic Press Inc., (1966).

17. H,M. Qiblawey and F. Banat, Solar thermal desalination technologies, *Desalination,* **220,** 633 (2008).

18. I. Shiklomanov, World fresh water resources, *Water in Crisis: A Guide to the World's Fresh Water Resources,* Oxford University Press, New York, (1993).

19. E.E. Delyannis and A. Delyannis, Economics of Solar Stills, *Desalination,* **52,** 167 (1985).

20. U.S. Centers for Disease Control and Prevention. Safe Water System: A Low-Cost Technology for Safe Drinking Water. *Fact Sheet, World Water Forum 4 Update*, (2006).

21. I.S. Al-Mutaz and M.I. Al-Ahmed, Evaluation of solar powered desalination processes, *Desalination,* **73**, 181 (1989).

22. M.K. Phadatare and S.K. Verma, Influence of water depth on internal heat and mass transfer in a plastic solar still, *Desalination,* **217**, 267 (2007).

23. Andrew Porteous, *Saline Water Distillation Processes*, Longman Group Limited, (1975).

24. G.O.G. Löf, Solar Distillation, Desalination Research and Water Resources, *Principles of Desalination*, Academic Press Inc., 1966.

25. S. Abdallah, O. Badran, M. M. Abu-Khader, Performance evaluation of a modified design of a single slope still, *Desalination,* **219**, 222 (2008).

26. O.A. Hamed, E.I. Eisa and W.E. Abdalla, Overview of solar desalination, *Desalination,* **93**, 47 (1993).

27. Murugavel, Chockalingam and Srithar, Progresses in improving the effectiveness of the single basin passive solar still, *Desalination,* **220**, 677 (2008).

28. K.K. Ettouney and Rizzuti, Solar Desalination: A challenge for sustainable fresh water in the 21st century, *Solar Desalination for the 21st Century*, Springer (2007).

29. M. Boukar and A. Harmim, Performance evaluation of a one-sided vertical solar still tested in the Desert of Algeria, *Desalination,* **183**, 113 (2005).

30. M.T. Chaibi, and K. Bourouni, Development of solar desalination systems concepts for irrigation in arid areas condition, *Solar Desalination for the 21st Century*, pp. 19, Springer, The Netherlands (2007).

31. K. Voropoulos, E. Mathioulakis, and V. Belessiotis, Experimental investigation of a solar still coupled with solar collectors, *Desalination,* **138**, 315 (2001).

32. E.D. Howe and B.W. Tleimat, Solar distillers for use on coral islands, *Desalination,* **2**, 109 (1967).

33. H.S. Aybar, A Review of Desalination by Solar Still, *Solar Desalination for the 21st Century*, pp. 207, Springer, The Netherlands, (2007).

34. G.N. Tiwari and V.S.V. Bapeshwara Rao, Transient performance of a single basin solar still with water flowing over the glass cover, *Desalination,* **49**, 231 (1984).

35. O.O. Badran, Experimental study of the enhancement parameters on a single slope solar still productivity, *Desalination*, **209**, 136 (2007).

36. G.M. Cappalletti, An experiment with a plastic solar still, *Desalination,* **147**, 221 (2002).

37. B.A.K. Abu-Hijleh, Enhanced solar still performance using water film cooling of the glass cover, *Desalination,* **107,** 235 (1996).

38. E.D. Howe, *Fundamentals of Water Desalination*, Marcel Dekker Inc., New York, (1974).

39. Y.P. Yadav and G.N. Tiwari, Monthly comparative performance of solar stills of various designs, *Desalination*, **67**, 565 (1987).

40. G.N. Tiwari and Madhuri, Effect of Water Depth on Daily Yield of the Still, *Desalination*, **61**, 67 (1987).

41. G.N. Tiwari, K. Mukherjee, K.R. Ashok, and Y.P. Yadav, Comparisons of various designs of solar stills, *Desalination,* **60**, 191 (1986).

42. S. Abdallah, M.M. Abu-Khader and O. Badran, Effect of various absorbing materials on the thermal performance of solar stills, *Desalination,* **242**, 128 (2009).

43. A.S. Nafey, M.A. Mohamad and M.A. Sharaf, Enhancement of solar water distillation process by surfactant additives, *Desalination,* **220**, 514 (2008).

44. G.N. Tiwari, Feasibility study of solar distillation plants in South Pacific countries, *Desalination,* **82**, 223 (1991).

45. J. Chenoweth, Minimum water requirement for social and economic development, *Desalination,* **229**, 245 (2008).